



HAL
open science

A Positive and Entropy-Satisfying Finite Volume Scheme for the Baer-Nunziato Model

Frédéric Coquel, Jean-Marc Hérard, Khaled Saleh

► **To cite this version:**

Frédéric Coquel, Jean-Marc Hérard, Khaled Saleh. A Positive and Entropy-Satisfying Finite Volume Scheme for the Baer-Nunziato Model. 2016. hal-01261458v2

HAL Id: hal-01261458

<https://hal.science/hal-01261458v2>

Preprint submitted on 10 Feb 2016 (v2), last revised 27 Oct 2016 (v4)

HAL is a multi-disciplinary open access archive for the deposit and dissemination of scientific research documents, whether they are published or not. The documents may come from teaching and research institutions in France or abroad, or from public or private research centers.

L'archive ouverte pluridisciplinaire **HAL**, est destinée au dépôt et à la diffusion de documents scientifiques de niveau recherche, publiés ou non, émanant des établissements d'enseignement et de recherche français ou étrangers, des laboratoires publics ou privés.



Distributed under a Creative Commons Attribution - NonCommercial - NoDerivatives 4.0 International License

A Positive and Entropy-Satisfying Finite Volume Scheme for the Baer-Nunziato Model

Frédéric Coquel¹, Jean-Marc Hérard², Khaled Saleh³

¹ CMAP, École Polytechnique CNRS, UMR 7641, Route de Saclay, F-91128 Palaiseau Cedex.

² EDF-R&D, Département MFEE, 6 Quai Watier, F-78401 Chatou Cedex, France.

³ Université de Lyon, CNRS UMR 5208, Université Lyon 1, Institut Camille Jordan, 43 bd 11 novembre 1918; F-69622 Villeurbanne cedex, France.

Abstract

We present a relaxation scheme for approximating the entropy dissipating weak solutions of the Baer-Nunziato two-phase flow model. This relaxation scheme is straightforwardly obtained as an extension of the relaxation scheme designed in [16] for the isentropic Baer-Nunziato model and consequently inherits its main properties. Up to our knowledge, this is the only existing scheme for which the approximated phase fractions, phase densities and phase pressures are proven to remain positive without any restrictive condition other than a classical fully computable CFL condition. It is also the only scheme for which a discrete entropy inequality is proven, under a CFL condition derived from the natural sub-characteristic condition associated with the relaxation approximation. These two properties of the numerical scheme (discrete positivity and entropy inequality) are satisfied for any admissible equation of state. We provide a numerical study for the convergence of the approximate solutions towards some exact Riemann solutions. The numerical simulations show a higher precision and a more reduced computational cost (for comparable accuracy) than standard numerical schemes used in the nuclear industry. We also assess the good behavior of the scheme when approximating vanishing phase solutions.

Key-words: Two-phase flows, energy-entropy duality, entropy-satisfying methods, relaxation techniques, Riemann problem.

AMS subject classifications: 76T05, 35L60, 35F55.

1 Introduction

The modeling and numerical simulation of two-phase flows is a relevant approach for a detailed investigation of some patterns occurring in water-vapor flows such as those encountered in nuclear power plants. The targeted applications are the normal operating mode of pressurized water reactors as well as incidental configurations such as the Departure from Nucleate Boiling (DNB) [42], the Loss of Coolant Accident (LOCA) [43], the re-flooding phase following a LOCA or the Reactivity Initiated Accident (RIA) [31]. In the normal operating mode, the flow in the primary circuit is quasi monophasic as there is *a priori* no vapor in the fluid. In the incidental configurations however, the vapor statistical fraction may take values ranging from zero to nearly one if some areas of the fluid have reached the boiling point. The modeling as well as the numerical simulation of such phenomena remains challenging since both models that can handle phase transitions and robust numerical schemes are needed. The derived schemes are expected to ensure important stability properties such as the positivity of the densities and pressures, as well as discrete entropy inequalities. In addition, as explicit schemes are needed for the simulation of these potentially highly unsteady phenomena, one major challenge is the control of the time step. In this context, the aim of this work is to design a robust and entropy-satisfying scheme for the numerical approximation of two-phase flows with vapor or liquid fractions arbitrarily close to zero.

The model concerned by this paper is the Baer-Nunziato two-phase flow model introduced in [9], and studied in various papers [20, 7, 12, 24, 33]. The model consists of two sets of partial differential equations accounting for the evolution of mass, momentum and total energy for each phase, in addition to a transport equation for the phase fraction. The evolution equations of the two phases are coupled through first order non-conservative terms depending on the phase fraction gradient. A major feature of the Baer-Nunziato model is to assume two different velocities and two different pressures for the two phases. This approach is not genuinely usual in the nuclear industry where the commonly implemented methods assume the same pressure for the two phases at every time and everywhere in the flow. This latter assumption is justified by the very short time-scale associated with the relaxation of the phasic pressures towards an equilibrium. In the two-fluid two-pressure models (such as Baer-Nunziato's), zero-th order source terms may be added in order to account for this pressure relaxation phenomenon as well as a drag force for the relaxation of the phasic velocities towards an equilibrium. However, this work is mainly concerned with the convective effects and these relaxation source terms are not considered here (see [12] for some modeling choices of these terms and [30] for their numerical treatment). Various models exist that are related to the Baer-Nunziato model. One may mention various closure laws for the interfacial velocity and pressure [23, 37, 25] or extensions to multi-phase flows [29, 27, 35].

Various approaches were considered to approximate the admissible weak solutions of the Baer-Nunziato model. One may mention exact Riemann solvers [38] or approximate Riemann solvers [5, 41, 6]. Let us mention some other schemes grounded on operator splitting techniques [11, 15, 34, 36, 39, 40, 18]. Let us also mention the original work of [3, 17] where two staggered grids are used (one for the scalar unknowns and the other for the velocities) and where the internal energies are discretized instead of the total energies.

The finite volume scheme we describe in the present paper relies on two main building blocks. The first block is a relaxation finite volume scheme previously designed in [16] for the isentropic version of the Baer-Nunziato model (the phasic entropies remain constant in both time and space along the process), a scheme which was proved to ensure positive densities and to satisfy discrete energy dissipation inequalities. The second building block is a duality principle between energy and entropy which, according to the second principle of thermodynamics states that, keeping all the other thermodynamic variables constant, the mathematical entropy is a decreasing function of the total energy. This duality principle was already used in previous works to extend schemes designed for the isentropic Euler equations to the full Euler equations (see [13] and [10]), and in this work, we apply these techniques to the Baer-Nunziato two-phase flow model. In [16], a relaxation Riemann solver was designed for the isentropic Baer-Nunziato model. The main properties of this scheme are firstly, to compute positive densities thanks to an energy dissipation process, secondly to satisfy discrete energy inequalities for each phase, and finally to compute robust approximations of vanishing phase cases where one (or both) of the phase fractions are arbitrarily close to zero in some areas of the flow. The fact that the phasic entropies are simply advected for smooth solutions of the Baer-Nunziato model, combined with the energy-entropy duality principle, actually allows us to use the very same Riemann solver designed in [16], provided that one supplements it with a correction step which consists in recovering the energy conservation and entropy dissipation for each phase.

Nevertheless, we draw the reader's attention on the fact that the relaxation scheme for the isentropic model, and its extension to the full model described here, are restricted to the simulations of flows with subsonic relative speeds, *i.e.* flows for which the difference between the material velocities of the phases is less than the speed of sound in the dominating phase, which would be the liquid phase in the usual operating of a nuclear power plant. For the simulation of nuclear liquid-vapor flows, this is not a restriction, but it would be interesting though to extend the present scheme to sonic and supersonic flows. An interesting work on this subject is done in [8].

The resulting scheme is proved to preserve positive phase fractions, densities and pressures, and to satisfy a discrete entropy inequality for each phase, under a sub-characteristic condition (Whitham's condition). To our knowledge, there exists no other scheme that is proved to satisfy these properties

altogether. In addition, for the same level of refinement, the scheme is shown to be much more accurate than the Rusanov scheme, and for a given level of approximation error, the relaxation scheme is shown to perform much better in terms of computational cost than this classical scheme. This is an important result because the approximate Riemann solver designed in [16] and re-used here relies on a fixed-point research for an increasing scalar function defined on the interval $(0, 1)$. Hence, the numerical tests assess that no heavy computational costs are due to this fixed-point research. Actually, comparing with Lax-Friedrichs type schemes is quite significant since for such stiff configurations as vanishing phase cases, these schemes are commonly used in the industrial context because of their known robustness [30]. Our relaxation scheme is first-order accurate and an interesting further work is the extension to higher orders (see [19, 41, 22] for examples of high order schemes).

The paper is organized as follows. Section 2 is devoted to the presentation of the Baer-Nunziato model. In Section 3, an auxiliary two-phase flow model is introduced, where the phasic entropies are conserved and the phasic total energies are dissipated. We explain how to extend the relaxation scheme designed in [16] to this auxiliary model. For the sake of completeness, the fully detailed Riemann solution is displayed in Section 7.1 of the appendix. In Section 4, we display the correction step which relies on the energy-entropy duality principle, and the resulting finite volume scheme for the Baer-Nunziato model is fully described. Finally, Section 5 is devoted to the numerical tests. In addition to a convergence and CPU cost study, one test case simulates a near-vacuum configuration, and two test-cases assess that the scheme provides a robust numerical treatment of vanishing phase solutions. For the reader who is eager to rapidly implement the numerical scheme, we refer to Section 7.2 of the appendix, where the procedure for computing the finite volume numerical fluxes is fully described.

2 The Baer-Nunziato model

The Baer-Nunziato model is a non-viscous two-phase flow model formulated in Eulerian coordinates and describing the evolution of the mass, momentum and total energy of each phase. Each phase is indexed by an integer $k \in \{1, 2\}$, the density of phase k is denoted ρ_k , its velocity u_k , and its specific total energy E_k . At each point x of the space and at each time t , the probability of finding phase k is denoted $\alpha_k(x, t)$. We assume the saturation constraint $\alpha_1 + \alpha_2 = 1$. In one-space dimension, the model reads:

$$\partial_t \mathcal{U} + \partial_x \mathcal{F}(\mathcal{U}) + \mathcal{C}(\mathcal{U}) \partial_x \mathcal{U} = 0, \quad x \in \mathbb{R}, t > 0, \quad (1)$$

where

$$\mathcal{U} = \begin{bmatrix} \alpha_1 \\ \alpha_1 \rho_1 \\ \alpha_2 \rho_2 \\ \alpha_1 \rho_1 u_1 \\ \alpha_2 \rho_2 u_2 \\ \alpha_1 \rho_1 E_1 \\ \alpha_2 \rho_2 E_2 \end{bmatrix}, \quad \mathcal{F}(\mathcal{U}) = \begin{bmatrix} 0 \\ \alpha_1 \rho_1 u_1 \\ \alpha_2 \rho_2 u_2 \\ \alpha_1 \rho_1 u_1^2 + \alpha_1 p_1 \\ \alpha_2 \rho_2 u_2^2 + \alpha_2 p_2 \\ \alpha_1 \rho_1 E_1 u_1 + \alpha_1 p_1 u_1 \\ \alpha_2 \rho_2 E_2 u_2 + \alpha_2 p_2 u_2 \end{bmatrix}, \quad \mathcal{C}(\mathcal{U}) \partial_x \mathcal{U} = \begin{bmatrix} u_2 \\ 0 \\ 0 \\ -p_1 \\ +p_1 \\ -p_1 u_2 \\ +p_1 u_2 \end{bmatrix} \partial_x \alpha_1. \quad (2)$$

The state vector \mathcal{U} is expected to belong to the natural physical space:

$$\Omega_{\mathcal{U}} = \{ \mathcal{U} \in \mathbb{R}^7, \alpha_1 \in (0, 1), \alpha_k \rho_k > 0, \text{ and } E_k - u_k^2/2 > 0 \text{ for } k \in \{1, 2\} \}. \quad (3)$$

For each $k \in \{1, 2\}$, p_k denotes the pressure of phase k . Defining $e_k := E_k - u_k^2/2$ the specific internal energy of phase k , the pressure is given by an equation of state (e.o.s.) as a function of e_k and the phasic density ρ_k . The mapping $(\rho_k, e_k) \mapsto p_k(\rho_k, e_k)$ is assumed to satisfy the natural properties $p_k(\rho_k, e_k) > 0$, $\partial_{\rho_k} p_k(\rho_k, e_k) > 0$ and $\partial_{e_k} p_k(\rho_k, e_k) > 0$ for all $\rho_k, e_k > 0$.

We assume that, taken separately, the two phases follow the second principle of thermodynamics so that for each phase $k \in \{1, 2\}$, there exists a positive integrating factor $T_k(\rho_k, e_k)$ such that the following differential form

$$\frac{1}{T_k} \left(\frac{p_k}{\rho_k^2} d\rho_k - de_k \right), \quad (4)$$

is the exact differential of some *strictly convex* function $s_k(\rho_k, e_k)$, called the (mathematical) entropy of phase k .

The following proposition characterizes the wave structure of this system:

Proposition 2.1. *System (1) is weakly hyperbolic on $\Omega_{\mathcal{U}}$ in the following sense. For all $\mathcal{U} \in \Omega_{\mathcal{U}}$, the Jacobian matrix $\mathcal{F}'(\mathcal{U}) + \mathcal{C}(\mathcal{U})$ admits seven real eigenvalues*

$$\begin{aligned} \sigma_1(\mathcal{U}) &= \sigma_2(\mathcal{U}) = u_2, \quad \sigma_3(\mathcal{U}) = u_1 \\ \sigma_4(\mathcal{U}) &= u_1 - c_1(\rho_1, e_1), \quad \sigma_5(\mathcal{U}) = u_1 + c_1(\rho_1, e_1) \\ \sigma_6(\mathcal{U}) &= u_2 - c_2(\rho_2, e_2), \quad \sigma_7(\mathcal{U}) = u_2 + c_2(\rho_2, e_2), \end{aligned} \quad (5)$$

where $c_k(\rho_k, e_k)^2 = \partial_{\rho_k} p_k(\rho_k, e_k) + p_k(\rho_k, e_k) / \rho_k^2 \partial_{e_k} p_k(\rho_k, e_k)$ is the speed of sound for phase k . The corresponding right eigenvectors are linearly independent if, and only if,

$$\alpha_1 \neq 0, \quad \alpha_2 \neq 0, \quad |u_1 - u_2| \neq c_1(\rho_1, e_1). \quad (6)$$

When (6) is not satisfied, the system is said to be **resonant**. The characteristic fields associated with $\sigma_4, \sigma_5, \sigma_6$ and σ_7 are genuinely non-linear, while the characteristic fields associated with $\sigma_{1,2}$ and σ_3 are linearly degenerate.

Remark 2.1. *The system is not hyperbolic in the usual sense because when (6) is not satisfied, the right eigenvectors do not span the whole space \mathbb{R}^7 . Two possible phenomena may cause a loss of the strict hyperbolicity: an interaction between the advective field of velocity u_2 with one of the acoustic fields of phase 1, and vanishing values of one of the phase fractions α_k . In the physical configurations aimed at in the present work (such as two-phase flows in nuclear reactors), the flows have strongly subsonic relative velocities, i.e. a relative Mach number much smaller than one:*

$$M = \frac{|u_1 - u_2|}{c_1(\rho_1, e_1)} \ll 1, \quad (7)$$

so that resonant configurations corresponding to wave interaction between acoustic fields and the u_2 -contact discontinuity are unlikely to occur. In addition, following the definition of the admissible physical space $\Omega_{\mathcal{U}}$, one never has $\alpha_1 = 0$ or $\alpha_2 = 0$. However, $\alpha_k = 0$ is to be understood in the sense $\alpha_k \rightarrow 0$ since one aim of this work is to construct a robust enough numerical scheme that could handle all the possible values of $\alpha_k, k \in \{1, 2\}$, especially, arbitrarily small values.

A simple computation shows that the smooth solutions of (1) also obey the following additional conservation laws on the phasic entropies:

$$\partial_t(\alpha_k \rho_k s_k) + \partial_x(\alpha_k \rho_k s_k u_k) = 0, \quad k \in \{1, 2\}. \quad (8)$$

As regards the non-smooth weak solutions of (1), one has to add a so-called *entropy criterion* in order to select the relevant physical solutions. In view of the convexity of the entropy $s_k(\rho_k, e_k)$, an entropy weak solution is a weak solution of (1) which satisfies the following entropy inequalities in the usual weak sense:

$$\partial_t(\alpha_k \rho_k s_k) + \partial_x(\alpha_k \rho_k s_k u_k) \leq 0, \quad k \in \{1, 2\}. \quad (9)$$

When the solution contains shock waves, inequalities (9) are strict in order to account for the physical loss of entropy due to viscous phenomena that are not modeled in system (1).

The existence of the phasic entropy conservation laws (8) and (9) will play a central role in the numerical approximation of the solutions of the Baer-Nunziato model. They permit an energy-entropy duality principle which allows to naturally extend to the non-isentropic model (1) the energy-dissipative relaxation scheme designed for the isentropic model in [16].

For the sake of completeness, let us recall the system of PDEs corresponding to the isentropic model: for $x \in \mathbb{R}, t > 0$:

$$\begin{aligned}
\partial_t \alpha_1 + u_2 \partial_x \alpha_1 &= 0, \\
\partial_t(\alpha_1 \rho_1) + \partial_x(\alpha_1 \rho_1 u_1) &= 0, \\
\partial_t(\alpha_1 \rho_1 u_1) + \partial_x(\alpha_1 \rho_1 u_1^2 + \alpha_1 p_1(\tau_1)) - p_1(\tau_1) \partial_x \alpha_1 &= 0, \\
\partial_t(\alpha_2 \rho_2) + \partial_x(\alpha_2 \rho_2 u_2) &= 0, \\
\partial_t(\alpha_2 \rho_2 u_2) + \partial_x(\alpha_2 \rho_2 u_2^2 + \alpha_2 p_2(\tau_2)) - p_2(\tau_2) \partial_x \alpha_2 &= 0.
\end{aligned} \tag{10}$$

In this case, the phasic pressures are functions solely of the phasic specific volumes $p_k(\tau_k)$, where $\tau_k = \rho_k^{-1}$, and the admissible weak solutions are seen to dissipate the phasic energies according to:

$$\partial_t(\alpha_k \rho_k E_k) + \partial_x(\alpha_k \rho_k E_k u_k + \alpha_k p_k(\tau_k) u_k) - u_2 p_1(\tau_1) \partial_x \alpha_k \leq 0, \quad k \in \{1, 2\}, \tag{11}$$

with $E_k = u_k^2/2 + e_k(\tau_k)$ where e_k is an anti-derivative of $-p_k$.

In a previous work [16], a relaxation scheme was designed for this isentropic Baer-Nunziato model. This scheme was proved to satisfy enjoyable properties such as maintaining positive phase fractions and densities, ensuring discrete counterparts of the energy inequalities (11), and finally computing with robustness solutions where some phase fractions are arbitrarily close to zero.

3 Approximating the weak solutions of an auxiliary model

As an intermediate step towards the purpose of approximating the entropy weak solutions of (1), let us introduce the following auxiliary system

$$\partial_t \mathbb{U} + \partial_x \mathbb{F}(\mathbb{U}) + \mathbb{C}(\mathbb{U}) \partial_x \mathbb{U} = 0, \quad x \in \mathbb{R}, t > 0, \tag{12}$$

where

$$\mathbb{U} = \begin{bmatrix} \alpha_1 \\ \alpha_1 \rho_1 \\ \alpha_2 \rho_2 \\ \alpha_1 \rho_1 u_1 \\ \alpha_2 \rho_2 u_2 \\ \alpha_1 \rho_1 s_1 \\ \alpha_2 \rho_2 s_2 \end{bmatrix}, \quad \mathbb{F}(\mathbb{U}) = \begin{bmatrix} 0 \\ \alpha_1 \rho_1 u_1 \\ \alpha_2 \rho_2 u_2 \\ \alpha_1 \rho_1 u_1^2 + \alpha_1 \mathcal{P}_1 \\ \alpha_2 \rho_2 u_2^2 + \alpha_2 \mathcal{P}_2 \\ \alpha_1 \rho_1 s_1 u_1 \\ \alpha_2 \rho_2 s_2 u_2 \end{bmatrix}, \quad \mathbb{C}(\mathbb{U}) \partial_x \mathbb{U} = \begin{bmatrix} u_2 \\ 0 \\ 0 \\ -\mathcal{P}_1 \\ +\mathcal{P}_1 \\ 0 \\ 0 \end{bmatrix} \partial_x \alpha_1. \tag{13}$$

Compared to the classical Baer-Nunziato model (1), the phasic energy equations have been replaced by the two conservation laws for the phasic entropies. Hence, $\alpha_k \rho_k s_k$ now play the role of independent conservative variables whose evolution is governed according to their own conservative equations. The phasic pressures \mathcal{P}_k are now seen as functions of the phasic specific volumes $\tau_k = \rho_k^{-1}$ and the phasic entropies s_k so that $\mathcal{P}_k = \mathcal{P}_k(\tau_k, s_k)$.

The auxiliary state vector \mathbb{U} is now expected to belong to the physical space:

$$\Omega_{\mathbb{U}} = \{ \mathbb{U} \in \mathbb{R}^7, \alpha_1 \in (0, 1), \alpha_k \rho_k > 0, \text{ and } \alpha_k \rho_k s_k > 0 \text{ for } k \in \{1, 2\} \}. \tag{14}$$

Actually, the entropy is usually defined up to a constant, however, we assume that $s_k > 0$ is a sufficient condition to uniquely define the internal energy in the following way: for fixed τ_k and s_k , the phasic internal energy $e_k(\tau_k, s_k)$ is defined as the (assumed unique) positive number e satisfying $p_k(\tau_k^{-1}, e) = \mathcal{P}_k(\tau_k, s_k)$, and the phasic total energy is recovered by computing $E_k(u_k, \tau_k, s_k) = u_k^2/2 + e_k(\tau_k, s_k)$.

With these thermodynamic relations, one may state the following property:

Proposition 3.1. *The two following equivalent assertions are satisfied :*

(i) The mapping

$$(\alpha_k \rho_k s_k) : \begin{cases} \Omega_{\mathcal{U}} & \longrightarrow \mathbb{R}^+ \\ \mathcal{U} & \longmapsto (\alpha_k \rho_k s_k)(\mathcal{U}) \end{cases}$$

satisfies $\partial_{\alpha_k \rho_k E_k}(\alpha_k \rho_k s_k)(\mathcal{U}) = -1/T_k$ and is convex.

(ii) The mapping

$$(\alpha_k \rho_k E_k) : \begin{cases} \Omega_{\mathbb{U}} & \longrightarrow \mathbb{R}^+ \\ \mathbb{U} & \longmapsto (\alpha_k \rho_k E_k)(\mathbb{U}) \end{cases}$$

satisfies $\partial_{\alpha_k \rho_k s_k}(\alpha_k \rho_k E_k)(\mathbb{U}) = -T_k$ and is convex.

Proof. In order to compute the partial derivative of $(\alpha_k \rho_k s_k)(\mathcal{U})$ with respect to $\alpha_k \rho_k E_k$, let us calculate the differential of $\alpha_k \rho_k s_k$. Invoking the second law of thermodynamics $T_k ds_k = -de_k + p_k \rho_k^{-2} d\rho_k$ and the definition $e_k = E_k - u_k^2/2$ of the internal energy, we obtain:

$$\begin{aligned} T_k d(\alpha_k \rho_k s_k) &= (\alpha_k \rho_k) T_k ds_k + T_k s_k d(\alpha_k \rho_k) \\ &= -(\alpha_k \rho_k) de_k + p_k \rho_k^{-2} (\alpha_k \rho_k) d\rho_k + T_k s_k d(\alpha_k \rho_k) \\ &= -(\alpha_k \rho_k) de_k - p_k d\alpha_k + (p_k \rho_k^{-1} + T_k s_k) d(\alpha_k \rho_k) \\ &= -(\alpha_k \rho_k) dE_k + (\alpha_k \rho_k u_k) du_k - p_k d\alpha_k + (p_k \rho_k^{-1} + T_k s_k) d(\alpha_k \rho_k) \\ &= -(\alpha_k \rho_k) dE_k + u_k d(\alpha_k \rho_k u_k) - u_k^2 d(\alpha_k \rho_k) - p_k d\alpha_k + (p_k \rho_k^{-1} + T_k s_k) d(\alpha_k \rho_k) \\ &= -d(\alpha_k \rho_k E_k) + u_k d(\alpha_k \rho_k u_k) - p_k d\alpha_k + (E_k - u_k^2 + p_k \rho_k^{-1} + T_k s_k) d(\alpha_k \rho_k). \end{aligned}$$

For $k \in \{1, 2\}$, $\partial_{\alpha_k \rho_k E_k}(\alpha_k \rho_k s_k)(\mathcal{U})$ is the derivative of $\alpha_k \rho_k s_k$ with respect to $\alpha_k \rho_k E_k$ when keeping constant the variables $(\alpha_i, \alpha_i \rho_i, \alpha_i \rho_i u_i)$ for $i \in \{1, 2\}$, and the variable $\alpha_{3-k} \rho_{3-k} E_{3-k}$. Hence, $\partial_{\alpha_k \rho_k E_k}(\alpha_k \rho_k s_k)(\mathcal{U}) = -1/T_k$ and the same computation proves that $\partial_{\alpha_k \rho_k s_k}(\alpha_k \rho_k E_k)(\mathbb{U}) = -T_k$. The proof of the convexity of these two mappings relies on the convexity of the function $s_k(\rho_k, e_k)$. It follows lengthy calculations (see [26]). We admit this result. \square

Of course, smooth solutions of (12) also solve (1) in the classical sense, which implies that they share the same hyperbolic structure, but entropy weak solutions of (1) and (12) do differ. Indeed, following Proposition 3.1, since $\mathbb{U} \mapsto (\alpha_k \rho_k E_k)(\mathbb{U})$ is convex, while the entropy weak solutions of (1) are defined so as to dissipate the phasic entropies, it turns natural to select weak solutions of the hyperbolic model (12) according to the differential inequalities:

$$\partial_t(\alpha_k \rho_k E_k) + \partial_x(\alpha_k \rho_k E_k u_k + \alpha_k \mathcal{P}_k(\tau_k, s_k) u_k) - \mathcal{P}_1(\tau_1, s_1) u_2 \partial_x \alpha_k \leq 0, \quad k \in \{1, 2\}. \quad (15)$$

Observe that for constant initial entropies $s_k(x, 0) = s_k^0$, the auxiliary model (12) reduces to the isentropic model (10), with the pressure laws $\tau_k \mapsto \mathcal{P}(\tau_k, s_k^0)$. Therefore, in the case of constant entropies, extending the relaxation scheme designed in [16] to the auxiliary model (12) is straightforward. Furthermore, even for non constant initial entropies, the derivation of the self-similar solutions for (12) is very close to the isentropic setting because the specific entropies are now just advected by the corresponding phase velocity:

$$\partial_t s_k + u_k \partial_x s_k = 0, \quad k \in \{1, 2\}. \quad (16)$$

For this reason, the Riemann solutions of the auxiliary model (12) are simpler to approximate than those of (1). But again, if smooth solutions of (1) and (12) are the same, their shock solutions are distinct. Hence, a numerical scheme for advancing in time discrete solutions of the original PDEs (1)–(9) based on solving a sequence of Riemann solutions for the auxiliary model (12)–(15) must be given a correction which enforces an energy discretization which is consistent with the original model (1), while ensuring discrete entropy inequalities consistently with (9). The required correction step turns in fact immediate because of the general thermodynamic assumptions made on the complete equation of state. It relies on a duality principle in between energy and entropy, which, according to Proposition 3.1, states that $\alpha_k \rho_k s_k$ is a decreasing function of $\alpha_k \rho_k E_k$.

In the present section, we provide a relaxation scheme for approximating the energy dissipating weak solutions of the auxiliary system (12). This relaxation scheme is straightforwardly obtained as an extension of the relaxation scheme designed in [16] for the isentropic Baer-Nunziato model and consequently inherits its main properties (positivity of the phase fractions and densities, numerical energy dissipation, robustness for vanishing phase fractions). Again this extension is made possible thanks to the advective equations (16) on the entropies. In Sections 3.1 and 3.2, we define the relaxation approximation for system (12) and state the existence theorem for the corresponding Riemann solver. This existence result, as it directly follows from the isentropic case, is not proven here. We refer the reader to [16] for the complete proof. In Section 3.3, we derive, thanks to this approximate Riemann solver, the numerical scheme for the auxiliary model (12). Finally, in Section 4, we explain how to obtain a positive an entropy-satisfying scheme for the original model (1), thanks to a duality principle between energy and entropy.

3.1 Relaxation approximation for the auxiliary model (12)

System (12) shares the same hyperbolic structure as system (1). Therefore, it has four genuinely non-linear fields associated with the phasic acoustic waves, which make the construction of an exact Riemann solver very difficult. In the spirit of [32], the relaxation approximation consists in considering an enlarged system involving two additional unknowns \mathcal{T}_k , associated with linearizations π_k of the phasic pressure laws. This linearization is designed to get a quasilinear enlarged system, shifting the initial non-linearity from the convective part to a stiff relaxation source term. The relaxation approximation is based on the idea that the solutions of the original system are formally recovered as the limit of the solutions of the proposed enlarged system, in the regime of a vanishing relaxation coefficient $\varepsilon > 0$. For a general framework on relaxation schemes we refer to [13, 14, 10].

We propose to approximate the Riemann problem for (12) by the self similar solution of the following Suliciu relaxation model:

$$\partial_t \mathbb{W}^\varepsilon + \partial_x \mathbf{g}(\mathbb{W}^\varepsilon) + \mathbf{d}(\mathbb{W}^\varepsilon) \partial_x \mathbb{W}^\varepsilon = \frac{1}{\varepsilon} \mathcal{R}(\mathbb{W}^\varepsilon), \quad x \in \mathbb{R}, t > 0, \quad (17)$$

with state vector $\mathbb{W} = (\alpha_1, \alpha_1 \rho_1, \alpha_2 \rho_2, \alpha_1 \rho_1 u_1, \alpha_2 \rho_2 u_2, \alpha_1 \rho_1 s_1, \alpha_2 \rho_2 s_2, \alpha_1 \rho_1 \mathcal{T}_1, \alpha_2 \rho_2 \mathcal{T}_2)^T$ and

$$\mathbf{g}(\mathbb{W}) = \begin{bmatrix} 0 \\ \alpha_1 \rho_1 u_1 \\ \alpha_2 \rho_2 u_2 \\ \alpha_1 \rho_1 u_1^2 + \alpha_1 \pi_1 \\ \alpha_2 \rho_2 u_2^2 + \alpha_2 \pi_2 \\ \alpha_1 \rho_1 s_1 u_1 \\ \alpha_2 \rho_2 s_2 u_2 \\ \alpha_1 \rho_1 \mathcal{T}_1 u_1 \\ \alpha_2 \rho_2 \mathcal{T}_2 u_2 \end{bmatrix}, \quad \mathbf{d}(\mathbb{W}) \partial_x \mathbb{W} = \begin{bmatrix} u_2 \\ 0 \\ 0 \\ -\pi_1 \\ \pi_1 \\ 0 \\ 0 \\ 0 \\ 0 \end{bmatrix} \partial_x \alpha_1, \quad \mathcal{R}(\mathbb{W}) = \begin{bmatrix} 0 \\ 0 \\ 0 \\ 0 \\ 0 \\ 0 \\ 0 \\ \alpha_1 \rho_1 (\tau_1 - \mathcal{T}_1) \\ \alpha_2 \rho_2 (\tau_2 - \mathcal{T}_2) \end{bmatrix}. \quad (18)$$

For each phase k in $\{1, 2\}$ the pressure π_k is a (partially) linearized pressure $\pi_k(\tau_k, \mathcal{T}_k, s_k)$ whose equation of state is defined by

$$\pi_k(\tau_k, \mathcal{T}_k, s_k) = \mathcal{P}_k(\mathcal{T}_k, s_k) + a_k^2 (\mathcal{T}_k - \tau_k). \quad (19)$$

In the formal limit $\varepsilon \rightarrow 0$, the additional variable \mathcal{T}_k tends towards the specific volume τ_k , and the linearized pressure law $\pi_k(\tau_k, \mathcal{T}_k, s_k)$ tends towards the original non-linear pressure law $\mathcal{P}_k(\tau_k, s_k)$, thus recovering system (12) in the first seven equations of (17). The solution of (17) should be parametrized by ε . However, in order to ease the notation, we omit the superscript $^\varepsilon$ in \mathbb{W}^ε . The constants a_k in (19) are two positive parameters that must be taken large enough so as to satisfy the following sub-characteristic condition (also called Whitham's condition):

$$a_k^2 > -\partial_{\tau_k} \mathcal{P}_k(\mathcal{T}_k, s_k), \quad k \text{ in } \{1, 2\}, \quad (20)$$

for all \mathcal{T}_k and s_k encountered in the solution of (17). Performing a Chapman-Enskog expansion, we can see that Whitham's condition expresses that system (17) is a viscous perturbation of system (12) in the regime of small ε . In addition, there exists two energy functionals $\mathcal{E}_k(u_k, \tau_k, \mathcal{T}_k, s_k)$, which under Whitham's condition, provide an H -theorem like result as stated in

Proposition 3.2. *The smooth solutions of (17) satisfy the following energy equations*

$$\partial_t(\alpha_k \rho_k \mathcal{E}_k) + \partial_x(\alpha_k \rho_k \mathcal{E}_k u_k + \alpha_k \pi_k u_k) - u_2 \pi_1 \partial_x \alpha_k = \frac{1}{\varepsilon} \alpha_k \rho_k (a_k^2 + \partial_{\tau_k} \mathcal{P}_k(\mathcal{T}_k, s_k)) (\tau_k - \mathcal{T}_k)^2, \quad (21)$$

where

$$\mathcal{E}_k := \mathcal{E}_k(u_k, \tau_k, \mathcal{T}_k, s_k) = \frac{u_k^2}{2} + e_k(\mathcal{T}_k, s_k) + \frac{\pi_k^2(\tau_k, \mathcal{T}_k, s_k) - \mathcal{P}_k^2(\mathcal{T}_k, s_k)}{2a_k^2}, \quad k \in \{1, 2\}. \quad (22)$$

Under Whitham's condition (20), to be met for all the (\mathcal{T}_k, s_k) under consideration, the following Gibbs principles are satisfied for $k \in \{1, 2\}$:

$$\tau_k = \underset{\mathcal{T}_k}{\text{Arg min}} \{ \mathcal{E}_k(u_k, \tau_k, \mathcal{T}_k, s_k) \}, \quad \text{and} \quad \mathcal{E}_k(u_k, \tau_k, \tau_k, s_k) = E_k(u_k, \tau_k, s_k). \quad (23)$$

At the numerical level, a fractional step method is commonly used in the implementation of relaxation methods: the first step is a time-advancing step using the solution of the Riemann problem for the convective part of (17):

$$\partial_t \mathbb{W} + \partial_x \mathbf{g}(\mathbb{W}) + \mathbf{d}(\mathbb{W}) \partial_x \mathbb{W} = 0, \quad (24)$$

while the second step consists in an instantaneous relaxation towards the equilibrium system by imposing $\mathcal{T}_k = \tau_k$ in the solution obtained by the first step. This second step is equivalent to sending ε to 0 instantaneously. As a consequence, we now focus on constructing an exact Riemann solver for the homogeneous convective system (24). Let us first state the main mathematical properties of the convective system (24), the solutions of which are sought in the domain of positive densities ρ_k and entropies s_k and positive \mathcal{T}_k :

$$\Omega_{\mathbb{W}} = \left\{ \mathbb{W} \in \mathbb{R}^7, 0 < \alpha_1 < 1, \alpha_k \rho_k > 0, \alpha_k \rho_k s_k > 0, \alpha_k \rho_k \mathcal{T}_k > 0, \text{ for } k \in \{1, 2\} \right\}. \quad (25)$$

Proposition 3.3. *System (24) is weakly hyperbolic on $\Omega_{\mathbb{W}}$ in the following sense. For all $\mathbb{W} \in \Omega_{\mathbb{W}}$, the Jacobian matrix $\mathbf{g}'(\mathbb{W}) + \mathbf{d}(\mathbb{W})$ admits the following real eigenvalues*

$$\begin{aligned} \sigma_1(\mathbb{W}) &= \sigma_2(\mathbb{W}) = \sigma_3(\mathbb{W}) = u_2, \quad \sigma_4(\mathbb{W}) = \sigma_5(\mathbb{W}) = u_1, \\ \sigma_6(\mathbb{W}) &= u_1 - a_1 \tau_1, \quad \sigma_7(\mathbb{W}) = u_1 + a_1 \tau_1, \\ \sigma_8(\mathbb{W}) &= u_2 - a_2 \tau_2, \quad \sigma_9(\mathbb{W}) = u_2 + a_2 \tau_2. \end{aligned} \quad (26)$$

All the characteristic fields associated with these eigenvalues are linearly degenerate and the corresponding right eigenvectors are linearly independent if, and only if

$$\alpha_1 \neq 0, \quad \alpha_2 \neq 0, \quad |u_1 - u_2| \neq a_1 \tau_1. \quad (27)$$

The smooth solutions of system (24) satisfy the following phasic energy equations:

$$\partial_t(\alpha_k \rho_k \mathcal{E}_k) + \partial_x(\alpha_k \rho_k \mathcal{E}_k u_k + \alpha_k \pi_k u_k) - u_2 \pi_1 \partial_x \alpha_k = 0. \quad (28)$$

Summing over $k \in \{1, 2\}$, the smooth solutions are seen to conserve the total mixture energy:

$$\partial_t \left(\sum_{k=1}^2 \alpha_k \rho_k \mathcal{E}_k \right) + \partial_x \left(\sum_{k=1}^2 (\alpha_k \rho_k \mathcal{E}_k u_k + \alpha_k \pi_k u_k) \right) = 0. \quad (29)$$

Remark 3.1. We look for subsonic solutions which are solutions that remain in the domain of $\Omega_{\mathbb{W}}$ where $|u_1 - u_2| < a_1\tau_1$. Here again, one never has $\alpha_1 = 0$ or $\alpha_2 = 0$. However, $\alpha_k = 0$ is to be understood in the sense $\alpha_k \rightarrow 0$.

Remark 3.2. Since all the characteristic fields of system (24) are linearly degenerate, the mixture energy equation (29) is expected to be satisfied for not only smooth but also weak solutions. However, in the stiff cases of vanishing phases where one of the left or right phase fractions $\alpha_{k,L}$ or $\alpha_{k,R}$ is close to zero, ensuring positive values of the densities requires an extra dissipation of the mixture energy by the computed solution (see the comments on Definition 3.1 below).

3.2 The relaxation Riemann problem

Let $(\mathbb{W}_L, \mathbb{W}_R)$ be two elements of $\Omega_{\mathbb{W}}$. We now consider the Cauchy problem for (24) with the following Riemann type initial data:

$$\mathbb{W}(x, 0) = \begin{cases} \mathbb{W}_L & \text{if } x < 0, \\ \mathbb{W}_R & \text{if } x > 0. \end{cases} \quad (30)$$

Extending the relaxation Riemann solution computed in [16, Section 3] for the isentropic setting to the present Riemann problem (24)-(30) follows from the crucial observation that both the relaxation volume fraction \mathcal{T}_k and the specific entropy s_k are advected in the same way by the phasic flow velocity u_k :

$$\begin{cases} \partial_t \mathcal{T}_k + u_k \partial_x \mathcal{T}_k = 0, \\ \partial_t s_k + u_k \partial_x s_k = 0. \end{cases} \quad (31)$$

Therefore, for self-similar initial data, the Riemann solution, as soon as it exists, necessarily obeys

$$\mathcal{T}_k(\xi) = \begin{cases} \mathcal{T}_{k,L}, & \xi < u_k^* \\ \mathcal{T}_{k,R}, & u_k^* < \xi, \end{cases} \quad s_k(\xi) = \begin{cases} s_{k,L}, & \xi < u_k^* \\ s_{k,R}, & u_k^* < \xi, \end{cases} \quad (32)$$

where $\xi = x/t$ is the self-similar variable, and u_k^* is the effective propagation speed associated with the eigenvalue u_k in the Riemann solution. Furthermore, any given combination of these variables, say $\phi(\mathcal{T}_k, s_k)$, is also advected by u_k . Hence, we obtain from (32), that the non-linear laws arising from the equation of state evolve in the Riemann solution, virtually the same way as within the isentropic setting. Indeed, the entropies s_k in the relaxation model (24) and in the associated energies (22), are systematically involved in non-linear functions already depending on the variable \mathcal{T}_k : namely $\mathcal{P}_k(\mathcal{T}_k, s_k)$ and $e_k(\mathcal{T}_k, s_k)$. Such functions are solely evaluated on the left and right states in the self-similar initial data and hence always contribute to any given jump conditions in terms of $\mathcal{P}_k(\mathcal{T}_{k,L}, s_{k,L})$, $e_k(\mathcal{T}_{k,L}, s_{k,L})$, $\mathcal{P}_k(\mathcal{T}_{k,R}, s_{k,R})$ or $e_k(\mathcal{T}_{k,R}, s_{k,R})$. For instance, computing the value of the linearized pressure $\pi_k(\xi)$ at some point ξ of the Riemann fan goes as follows:

$$\pi_k(\xi) = \pi_k(\tau_k(\xi), \mathcal{T}_k(\xi), s_k(\xi)) = \mathcal{P}_k(\mathcal{T}_k(\xi), s_k(\xi)) + a_k^2(\mathcal{T}_k(\xi) - \tau_k(\xi)),$$

where $\mathcal{P}_k(\mathcal{T}_k(\xi), s_k(\xi)) = \mathcal{P}_k(\mathcal{T}_{k,L}, s_{k,L})$ if $\xi < u_k^*$ and $\mathcal{P}_k(\mathcal{T}_k(\xi), s_k(\xi)) = \mathcal{P}_k(\mathcal{T}_{k,R}, s_{k,R})$ otherwise, whereas in the isentropic setting, one would have $\mathcal{P}_k(\mathcal{T}_{k,L})$ or $\mathcal{P}_k(\mathcal{T}_{k,R})$. The same observations can be made for the internal energy $e_k(\mathcal{T}_k, s_k)$ when computing the total energy $\mathcal{E}_k(u_k(\xi), \tau_k(\xi), \mathcal{T}_k(\xi), s_k(\xi))$. Hence, compared to the isentropic case, it is just as if the relaxation unknown \mathcal{T}_k is replaced by a two-dimensional vector (\mathcal{T}_k, s_k) . We formalize these observations in

Proposition 3.4. Let $(\mathbb{W}_L, \mathbb{W}_R) \in \Omega_{\mathbb{W}} \times \Omega_{\mathbb{W}}$. The Riemann problem (24)-(30) admits a solution if, and only if, the isentropic Riemann problem obtained when taking constant initial entropies $s_{k,L} = s_{k,R}$, $k \in \{1, 2\}$ while keeping the other initial data unchanged, admits a solution. When such a solution exists, the mathematical formulae for defining the phasic quantities τ_k, u_k, π_k, e_k and the void fraction α_k within the Riemann fan read exactly the same as in the isentropic framework [16, Section 3], provided the following replacements:

$$\begin{aligned} \mathcal{P}_k(\mathcal{T}_{k,L}) &\longrightarrow \mathcal{P}_k(\mathcal{T}_{k,L}, s_{k,L}), & \mathcal{P}_k(\mathcal{T}_{k,R}) &\longrightarrow \mathcal{P}_k(\mathcal{T}_{k,R}, s_{k,R}), \\ e_k(\mathcal{T}_{k,L}) &\longrightarrow e_k(\mathcal{T}_{k,L}, s_{k,L}), & e_k(\mathcal{T}_{k,R}) &\longrightarrow e_k(\mathcal{T}_{k,R}, s_{k,R}). \end{aligned} \quad (33)$$

In the following definition, we recall the main features of a solution to the Riemann problem (24)-(30).

Definition 3.1. Let $(\mathbb{W}_L, \mathbb{W}_R)$ be two states in $\Omega_{\mathbb{W}}$. A solution to the Riemann problem (24)-(30) **with subsonic wave ordering** is a self-similar mapping $\mathbb{W}(x, t) = \mathbb{W}_r(x/t; \mathbb{W}_L, \mathbb{W}_R)$ where the function $\xi \mapsto \mathbb{W}_r(\xi; \mathbb{W}_L, \mathbb{W}_R)$ satisfies the following properties:

- (i) $\mathbb{W}_r(\xi; \mathbb{W}_L, \mathbb{W}_R)$ is a piecewise constant function, composed of (at most) seven intermediate states belonging to $\Omega_{\mathbb{W}}$, separated by (at most) six contact discontinuities associated with the eigenvalues $u_1 \pm a_1\tau_1$, $u_2 \pm a_2\tau_2$, u_1 , u_2 and such that

$$\begin{aligned} \xi < \min_{k \in \{1,2\}} \{u_{k,L} - a_k\tau_{k,L}\} &\implies \mathbb{W}_r(\xi; \mathbb{W}_L, \mathbb{W}_R) = \mathbb{W}_L, \\ \xi > \max_{k \in \{1,2\}} \{u_{k,R} + a_k\tau_{k,R}\} &\implies \mathbb{W}_r(\xi; \mathbb{W}_L, \mathbb{W}_R) = \mathbb{W}_R. \end{aligned} \quad (34)$$

- (ii) There exists two real numbers u_2^* and π_1^* (depending on $(\mathbb{W}_L, \mathbb{W}_R)$) such that the function $\mathbb{W}(x, t) = \mathbb{W}_r(x/t; \mathbb{W}_L, \mathbb{W}_R)$ satisfies the following PDEs in the distributional sense: for $k \in \{1, 2\}$,

$$\partial_t \alpha_k + u_2^* \partial_x \alpha_k = 0, \quad (35)$$

$$\partial_t (\alpha_k \rho_k) + \partial_x (\alpha_k \rho_k u_k) = 0, \quad (36)$$

$$\partial_t (\alpha_k \rho_k u_k) + \partial_x (\alpha_k \rho_k u_k^2 + \alpha_k) - \pi_1^* \partial_x \alpha_k = 0, \quad (37)$$

$$\partial_t (\alpha_k \rho_k s_k) + \partial_x (\alpha_k \rho_k s_k u_k) = 0, \quad (38)$$

$$\partial_t (\alpha_k \rho_k \mathcal{T}_k) + \partial_x (\alpha_k \rho_k \mathcal{T}_k u_k) = 0, \quad (39)$$

where $\partial_x \alpha_k$ identifies with the Dirac measure $\Delta \alpha_k \delta_{x-u_2^*t}$, with $\Delta \alpha_k = \alpha_{k,R} - \alpha_{k,L}$.

- (iii) Furthermore, the function $\mathbb{W}(x, t) = \mathbb{W}_r(x/t; \mathbb{W}_L, \mathbb{W}_R)$ also satisfies the following energy equations in the distributional sense:

$$\partial_t (\alpha_2 \rho_2 \mathcal{E}_2) + \partial_x (\alpha_2 \rho_2 \mathcal{E}_2 u_2 + \alpha_2 \pi_2 u_2) - u_2^* \pi_1^* \partial_x \alpha_2 = 0, \quad (40)$$

$$\partial_t (\alpha_1 \rho_1 \mathcal{E}_1) + \partial_x (\alpha_1 \rho_1 \mathcal{E}_1 u_1 + \alpha_1 \pi_1 u_1) - u_2^* \pi_1^* \partial_x \alpha_1 = -\mathcal{Q}(u_2^*, \mathbb{W}_L, \mathbb{W}_R) \delta_{x-u_2^*t}, \quad (41)$$

where $\mathcal{Q}(u_2^*, \mathbb{W}_L, \mathbb{W}_R)$ is a nonnegative number.

- (iv) The solution has a **subsonic wave ordering** in the following sense:

$$u_{1,L} - a_1\tau_{1,L} < u_2^* < u_{1,R} + a_1\tau_{1,R}. \quad (42)$$

Before stating the existence theorem for subsonic solutions proved in [16, Section 3], let us introduce some notations built on the initial states $(\mathbb{W}_L, \mathbb{W}_R)$ and on the relaxation parameters (a_1, a_2) . For k in $\{1, 2\}$,

$$u_k^\# := \frac{1}{2} (u_{k,L} + u_{k,R}) - \frac{1}{2a_k} (\pi_k(\tau_{k,R}, \mathcal{T}_{k,R}, s_{k,R}) - \pi_k(\tau_{k,L}, \mathcal{T}_{k,L}, s_{k,L})), \quad (43)$$

$$\pi_k^\# := \frac{1}{2} (\pi_k(\tau_{k,R}, \mathcal{T}_{k,R}, s_{k,R}) + \pi_k(\tau_{k,L}, \mathcal{T}_{k,L}, s_{k,L})) - \frac{a_k}{2} (u_{k,R} - u_{k,L}), \quad (44)$$

$$\tau_{k,L}^\# := \tau_{k,L} + \frac{1}{a_k} (u_k^\# - u_{k,L}), \quad (45)$$

$$\tau_{k,R}^\# := \tau_{k,R} - \frac{1}{a_k} (u_k^\# - u_{k,R}). \quad (46)$$

We also introduce the following dimensionless number that only depends on the initial phase fractions:

$$\Lambda^\alpha := \frac{\alpha_{2,R} - \alpha_{2,L}}{\alpha_{2,R} + \alpha_{2,L}}. \quad (47)$$

We may now state the existence result for the Riemann problem (24)-(30), which is directly inferred from the existence Theorem for the solutions to the relaxation Riemann problem for the isentropic case designed in [16, Section 3]. The construction of the self-similar solution is fully displayed in Appendix 7.1.

Theorem 3.5. *Let be given a pair of admissible initial states $(\mathbb{W}_L, \mathbb{W}_R) \in \Omega_{\mathbb{W}} \times \Omega_{\mathbb{W}}$ and assume that the parameter a_k is such that $\tau_{k,L}^{\sharp} > 0$ and $\tau_{k,R}^{\sharp} > 0$ for k in $\{1, 2\}$. There exists solutions with subsonic wave ordering to the Riemann problem (24)-(30), in the sense of Definition 3.1, if the following condition holds:*

$$(A) \quad -a_1\tau_{1,R}^{\sharp} < \frac{u_1^{\sharp} - u_2^{\sharp} - \frac{1}{a_2}\Lambda^{\alpha}(\pi_1^{\sharp} - \pi_2^{\sharp})}{1 + \frac{a_1}{a_2}|\Lambda^{\alpha}|} < a_1\tau_{1,L}^{\sharp}.$$

Proof. Following Proposition 3.4, see [16, Section 3] for a constructive proof and the remarks below. See Appendix 7.1 for the expressions of the intermediate states of the solution. \square

Some comments on Definition 3.1 and Theorem 3.5:

1. Assumption (A) can be explicitly tested in terms of the initial data and the parameters a_k , $k \in \{1, 2\}$. The quantities $a_1\tau_{1,L}^{\sharp}$ and $a_1\tau_{1,R}^{\sharp}$ can be seen as two sound propagation speeds, while the quantity $(u_1^{\sharp} - u_2^{\sharp} - \frac{1}{a_2}\Lambda^{\alpha}(\pi_1^{\sharp} - \pi_2^{\sharp})) / (1 + \frac{a_1}{a_2}|\Lambda^{\alpha}|)$, which has the dimension of a velocity, measures the difference between the pressures and kinematic velocities of the two phases, in the initial data. Observe that if the initial data is close to the pressure and velocity equilibrium between the two phases, this quantity is expected to be small compared to $a_1\tau_{1,L}^{\sharp}$ and $a_1\tau_{1,R}^{\sharp}$. This is actually the case when, in addition to the convective system (1), zero-th order source terms are added to the model in order to account for relaxation phenomena that tend to bring the two phases towards thermodynamical ($T_1 = T_2$ and $u_1 = u_2$) and mechanical ($p_1 = p_2$) equilibria (see [12, 21] for the models and [30] for adapted numerical methods).
2. The quantity u_2^* is the propagation velocity of the phase fraction wave. It is computed as the zero of a monotone real function $z \mapsto \Psi_{(\mathbb{W}_L, \mathbb{W}_R)}(z)$ on a bounded interval. Assumption (A) is a sufficient and necessary condition for this function $\Psi_{(\mathbb{W}_L, \mathbb{W}_R)}$ to have a unique zero (*i.e.* a unique number u_2^* satisfying $\Psi_{(\mathbb{W}_L, \mathbb{W}_R)}(u_2^*) = 0$). Hence, solving this fixed-point problem enables to locate the phase fraction wave by coupling two monophasic systems. Let us stress again on the fact this fixed-point problem is very easy to solve numerically, since it boils down to searching the zero of a strictly monotone function on a bounded interval. We refer to equation (79) in appendix 7.1 and to the paper [16] for more details.
3. **Positivity of phase 1 densities.** If the ratio $\frac{\alpha_{1,L}}{\alpha_{1,R}}$ is in a neighborhood of 1, the solution computed thanks to condition (A) has positive densities and satisfies the phasic energy equations (28) in the weak sense. In this case, the solution is said to be energy-preserving and the total mixture energy is also conserved according to the conservative equation (29). If $\frac{\alpha_{1,L}}{\alpha_{1,R}}$ is too large, or too small, depending on the wave ordering between u_2^* and u_1^* , the solution computed thanks to condition (A) may have non-positive densities in phase 1. In such stiff cases, ensuring positive densities for phase 1 is recovered by allowing a strict dissipation of the phase 1 energy:

$$\partial_t(\alpha_1\rho_1\mathcal{E}_1) + \partial_x(\alpha_1\rho_1\mathcal{E}_1 + \alpha_1\pi_1)u_1 - u_2^*\pi_1^*\partial_x\alpha_1 = -\mathcal{Q}(u_2^*, \mathbb{W}_L, \mathbb{W}_R)\delta_{x-u_2^*t}, \quad (48)$$

where $\mathcal{Q}(u_2^*, \mathbb{W}_L, \mathbb{W}_R) < 0$. The function $\mathcal{Q}(u_2^*, \mathbb{W}_L, \mathbb{W}_R)$ is a **kinetic relation** which is chosen large enough so as to impose the positivity of all the phase 1 densities. The value of $\mathcal{Q}(u_2^*, \mathbb{W}_L, \mathbb{W}_R)$ parametrizes the whole solution and the choice of $\mathcal{Q}(u_2^*, \mathbb{W}_L, \mathbb{W}_R)$ prescribes a unique solution.

4. **Positivity of phase 2 densities.** Assumption (A) allows to compute the value of the wave propagation velocity u_2^* (see comment 2). With this value, one has to *verify* that the following property, which is equivalent to the positivity of the phase 2 densities, is satisfied:

$$(B) \quad u_2^{\sharp} - a_2\tau_{2,L}^{\sharp} < u_2^* < u_2^{\sharp} + a_2\tau_{2,R}^{\sharp}. \quad (49)$$

In the numerical applications using this Riemann solver (see Section 5), it will always be possible to ensure property **(B)** by taking a large enough value of the relaxation parameter a_2 (see Appendix 7.2). Note that this condition is a monophasic condition which is not related to the two-fluid modeling. Indeed, the same condition is required when approximating Euler's equations with a similar relaxation scheme.

5. **Positivity of the entropies.** The phasic entropies s_k , $k \in \{1, 2\}$ satisfy a maximum principle in the solution since they are simply advected by the phasic velocities according to (31). Hence, since at the initial time $s_{k,L} > 0$ and $s_{k,R} > 0$ for $k \in \{1, 2\}$, one has $s_k(\xi) > 0$ everywhere in the Riemann fan, for $k \in \{1, 2\}$.
6. For the applications aimed at by this work, such as nuclear flows, we are only interested in solutions which have a *subsonic wave ordering*, *i.e.* solutions for which the propagation velocity u_2^* of the phase fraction α_1 lies in-between the acoustic waves of phase 1, which is what is required in item (iv). However, the considered solutions are allowed to have **phasic supersonic speeds** $|u_k| > a_k \tau_k$. Indeed, the subsonic property considered here is related to the **relative velocity** $u_1 - u_2$ with respect to the phase 1 speed of sound $a_1 \tau_1$.

3.3 The relaxation scheme for the auxiliary model

In this section, the exact Riemann solver $\mathbb{W}_r(\xi; \mathbb{W}_L, \mathbb{W}_R)$ for the relaxation system (24) is used to derive an approximate Riemann solver of Harten, Lax and van Leer [28] for the simulation of the auxiliary system (12). The aim is to approximate the admissible weak solution of a Cauchy problem associated with system (12):

$$\begin{cases} \partial_t \mathbb{U} + \partial_x \mathbb{F}(\mathbb{U}) + \mathbb{C}(\mathbb{U}) \partial_x \mathbb{U} = 0, & x \in \mathbb{R}, t > 0, \\ \mathbb{U}(x, 0) = \mathbb{U}_0(x), & x \in \mathbb{R}, \end{cases} \quad (50)$$

with a discretization which provides discrete counterparts of the energy inequalities (15) satisfied by the exact solutions of the auxiliary model. As expected, the numerical scheme is identical to the relaxation scheme designed in [16] for the isentropic model.

We define a time and space discretization as follows: for simplicity in the notations, we assume constant positive time and space steps Δt and Δx , and we define $\lambda = \frac{\Delta t}{\Delta x}$. The space is partitioned into cells $\mathbb{R} = \bigcup_{j \in \mathbb{Z}} C_j$ where $C_j = [x_{j-\frac{1}{2}}, x_{j+\frac{1}{2}}[$ with $x_{j+\frac{1}{2}} = (j + \frac{1}{2})\Delta x$ for all j in \mathbb{Z} . The centers of the cells are denoted $x_j = j\Delta x$ for all j in \mathbb{Z} . We also introduce the discrete intermediate times $t^n = n\Delta t$, $n \in \mathbb{N}$. The approximate solution at time t^n , $x \in \mathbb{R} \mapsto \mathbb{U}_\lambda(x, t^n) \in \Omega$ is a piecewise constant function whose value on each cell C_j is a constant value denoted by \mathbb{U}_j^n . Since $\mathbb{U}_\lambda(x, t^n)$ is piecewise constant, the exact solution of the following Cauchy problem at time t^n

$$\begin{cases} \partial_t \mathbb{U} + \partial_x \mathbb{F}(\mathbb{U}) + \mathbb{C}(\mathbb{U}) \partial_x \mathbb{U} = 0, & x \in \mathbb{R}, t > 0, \\ \mathbb{U}(x, 0) = \mathbb{U}_\lambda(x, t^n), & x \in \mathbb{R}, \end{cases} \quad (51)$$

is obtained by juxtaposing the solutions of the Riemann problems set at each cell interface $x_{j+\frac{1}{2}}$, provided that these Riemann problems do not interact. The relaxation approximation is an approximate Riemann solver which consists in defining:

$$\mathbb{U}_j^{n+1} := \frac{1}{\Delta x} \int_{x_{j-\frac{1}{2}}}^{x_{j+\frac{1}{2}}} \mathbb{U}_{app}(x, \Delta t) dx,$$

where $\mathbb{U}_{app}(x, t)$ is following approximate solution of (51):

$$\mathbb{U}_{app}(x, t) := \sum_{j \in \mathbb{Z}} \mathcal{P} \mathbb{W}_r \left(\frac{x - x_{j+\frac{1}{2}}}{t}; \mathcal{M}(\mathbb{U}_j^n), \mathcal{M}(\mathbb{U}_{j+1}^n) \right) \mathbb{1}_{[x_j, x_{j+1}]}(x), \quad (52)$$

where the mappings \mathcal{P} and \mathcal{M} are defined by:

$$\mathcal{M} : \begin{cases} \mathbb{R}^7 & \longrightarrow \mathbb{R}^9 \\ (x_k)_{k=1,\dots,7} & \longmapsto (x_1, x_2, x_3, x_4, x_5, x_6, x_7, x_1, 1 - x_1). \end{cases} \quad (53)$$

$$\mathcal{P} : \begin{cases} \mathbb{R}^9 & \longrightarrow \mathbb{R}^7 \\ (x_k)_{k=1,\dots,9} & \longmapsto (x_1, x_2, x_3, x_4, x_5, x_6, x_7). \end{cases} \quad (54)$$

For a given vector \mathbb{U} , $\mathbb{W} = \mathcal{M}(\mathbb{U})$ is the relaxation vector obtained by keeping α_k , $\alpha_k \rho_k$, $\alpha_k \rho_k u_k$ and $\alpha_k \rho_k s_k$ unchanged, while setting \mathcal{T}_k to be equal to τ_k . One says that $\mathbb{W} \in \Omega_{\mathbb{W}}$ is at equilibrium if there exists $\mathbb{U} \in \Omega_{\mathbb{U}}$ such that $\mathbb{W} = \mathcal{M}(\mathbb{U})$. For a given relaxation vector \mathbb{W} , $\mathbb{U} = \mathcal{P}\mathbb{W}$ is the projection of \mathbb{W} which consists in dropping the relaxation unknowns \mathcal{T}_k .

In order for the interface Riemann problems not to interact and thus for $\mathbb{U}_{app}(x, t)$ to be a correct approximate solution of (51), the time step Δt is chosen small enough so as to satisfy the CFL condition

$$\frac{\Delta t}{\Delta x} \max_{k \in \{1,2\}, j \in \mathbb{Z}} \max \{ |(u_k - a_k \tau_k)_j^n|, |(u_k + a_k \tau_k)_{j+1}^n| \} < \frac{1}{2}. \quad (55)$$

Of course, at each interface $x_{j+\frac{1}{2}}$, the relaxation Riemann solver $\mathbb{W}_r(\xi; \mathcal{M}(\mathbb{U}_j^n), \mathcal{M}(\mathbb{U}_{j+1}^n))$ depends on two parameters $(a_k)_{j+\frac{1}{2}}^n, k \in \{1, 2\}$ which must be chosen so as to ensure the conditions stated in the existence Theorem 3.5, and to satisfy some stability properties. Observe that one might take different relaxation parameters $a_k, k \in \{1, 2\}$ for each interface, which amounts to approximating the equilibrium system (12) by a different relaxation approximation at each interface, which is more or less diffusive depending on how large are the local parameters $(a_k)_{j+\frac{1}{2}}^n, k \in \{1, 2\}$. We do not precise at this point the practical computation of these parameters. This discussion is postponed to Section 7.2 of the Appendices.

Since $\mathbb{W}_r(\xi; \mathbb{W}_L, \mathbb{W}_R)$ is the exact solution of the relaxation Riemann problem (24)-(30), the updated unknown \mathbb{U}_j^{n+1} may be computed by a non-conservative finite volume formula as stated in

Proposition 3.6. *Provided the CFL condition (55) is satisfied, the updated unknown \mathbb{U}_j^{n+1} is given by:*

$$\mathbb{U}_j^{n+1} = \mathbb{U}_j^n - \frac{\Delta t}{\Delta x} (\mathbf{F}^-(\mathbb{U}_j^n, \mathbb{U}_{j+1}^n) - \mathbf{F}^+(\mathbb{U}_{j-1}^n, \mathbb{U}_j^n)). \quad (56)$$

where the numerical fluxes read

$$\mathbf{F}^-(\mathbb{U}_L, \mathbb{U}_R) = \mathcal{P} \mathbf{g}(\mathbb{W}_r(0^-; \mathcal{M}(\mathbb{U}_L), \mathcal{M}(\mathbb{U}_R))) + \mathcal{P} \mathbf{D}^*(\mathcal{M}(\mathbb{U}_L), \mathcal{M}(\mathbb{U}_R)) \mathbf{1}_{\{u_2^* < 0\}}, \quad (57)$$

$$\mathbf{F}^+(\mathbb{U}_L, \mathbb{U}_R) = \mathcal{P} \mathbf{g}(\mathbb{W}_r(0^+; \mathcal{M}(\mathbb{U}_L), \mathcal{M}(\mathbb{U}_R))) - \mathcal{P} \mathbf{D}^*(\mathcal{M}(\mathbb{U}_L), \mathcal{M}(\mathbb{U}_R)) \mathbf{1}_{\{u_2^* > 0\}}, \quad (58)$$

with $\mathbf{D}^*(\mathbb{W}_L, \mathbb{W}_R) := (\alpha_{1,R} - \alpha_{1,L})(u_2^*(\mathbb{W}_L, \mathbb{W}_R), 0, 0, -\pi_1^*(\mathbb{W}_L, \mathbb{W}_R), \pi_1^*(\mathbb{W}_L, \mathbb{W}_R), 0, 0, 0, 0)^T$.

Proof. Under the CFL condition (55), the exact solution of (24) with the piecewise constant initial data $\mathbb{W}(x, 0) := \sum_{j \in \mathbb{Z}} \mathcal{M}(\mathbb{U}_j^n) \mathbf{1}_{[x_j, x_{j+1}]}(x)$ is the function:

$$\mathbb{W}(x, t) := \sum_{j \in \mathbb{Z}} \mathbb{W}_r\left(\frac{x - x_{j+\frac{1}{2}}}{t}; \mathcal{M}(\mathbb{U}_j^n), \mathcal{M}(\mathbb{U}_{j+1}^n)\right) \mathbf{1}_{[x_j, x_{j+1}]}(x),$$

since the interface Riemann problems do not interact. In addition, under (55), (24) may be written:

$$\partial_t \mathbb{W} + \partial_x \mathbf{g}(\mathbb{W}) + \sum_{j \in \mathbb{Z}} \mathbf{D}^*(\mathcal{M}(\mathbb{U}_j^n), \mathcal{M}(\mathbb{U}_{j+1}^n)) \delta_0 \left(x - x_{j+\frac{1}{2}} - (u_2^*)_{j+\frac{1}{2}}^n t \right) = 0,$$

where $\mathbf{D}^*(\mathbb{W}_L, \mathbb{W}_R)$ is defined in the proposition. Integrating this PDE over $(x_{j-\frac{1}{2}}, x_{j+\frac{1}{2}}) \times [0, \Delta t]$ and dividing by Δx , one obtains:

$$\begin{aligned} \frac{1}{\Delta x} \int_{x_{j-\frac{1}{2}}}^{x_{j+\frac{1}{2}}} \mathbb{W}(x, \Delta t) dx &= \mathcal{M}(\mathbb{U}_j^n) \\ &- \frac{\Delta t}{\Delta x} \left(\mathbf{g}(\mathbb{W}_r(0^-; \mathcal{M}(\mathbb{U}_j^n), \mathcal{M}(\mathbb{U}_{j+1}^n))) - \mathbf{g}(\mathbb{W}_r(0^+; \mathcal{M}(\mathbb{U}_{j-1}^n), \mathcal{M}(\mathbb{U}_j^n))) \right) \\ &- \frac{\Delta t}{\Delta x} \mathbf{D}^*(\mathcal{M}(\mathbb{U}_j^n), \mathcal{M}(\mathbb{U}_{j+1}^n)) \mathbf{1}_{\{(u_2^*)_{j+\frac{1}{2}}^n < 0\}} \\ &- \frac{\Delta t}{\Delta x} \mathbf{D}^*(\mathcal{M}(\mathbb{U}_{j-1}^n), \mathcal{M}(\mathbb{U}_j^n)) \mathbf{1}_{\{(u_2^*)_{j-\frac{1}{2}}^n > 0\}}. \end{aligned}$$

Applying operator \mathcal{P} to this equation yields (56). \square

This approximate Riemann solver is proved to ensure a conservative discretization of the partial masses, partial entropies and total mixture momentum and to satisfy important stability properties such as the preservation of the densities and entropies positivity, and discrete energy inequalities which are discrete counterparts of the energy inequalities (28) satisfied by the exact weak solutions of the model. Indeed, we have the following result:

Proposition 3.7. *The numerical scheme (56) for the auxiliary model has the following properties:*

- **Positivity:** *Under the CFL condition (55), for all $n \in \mathbb{N}$, if $\mathbb{U}_j^n \in \Omega_{\mathbb{U}}$ for all $j \in \mathbb{Z}$, then $0 < (\alpha_k)_j^{n+1} < 1$, $(\alpha_k \rho_k)_j^{n+1} > 0$, and $(\alpha_k \rho_k s_k)_j^{n+1} > 0$ for $k = 1, 2$ and all $j \in \mathbb{Z}$, i.e. $\mathbb{U}_j^{n+1} \in \Omega_{\mathbb{U}}$ for all $j \in \mathbb{Z}$.*

- **Phasic mass conservation:** *Denoting \mathbf{F}_i^\pm the i^{th} component of vector \mathbf{F}^\pm , the fluxes for the phasic partial masses $\alpha_k \rho_k$ are conservative: $\mathbf{F}_i^-(\mathbb{U}_L, \mathbb{U}_R) = \mathbf{F}_i^+(\mathbb{U}_L, \mathbb{U}_R)$ for i in $\{2, 3\}$. Hence, denoting $(\alpha_k \rho_k u_k)_{j+\frac{1}{2}}^n = \mathbf{F}_{1+k}^\pm(\mathbb{U}_j^n, \mathbb{U}_{j+1}^n)$ for $k = 1, 2$, one has:*

$$(\alpha_k \rho_k)_j^{n+1} = (\alpha_k \rho_k)_j^n - \frac{\Delta t}{\Delta x} \left((\alpha_k \rho_k u_k)_{j+\frac{1}{2}}^n - (\alpha_k \rho_k u_k)_{j-\frac{1}{2}}^n \right). \quad (59)$$

- **Phasic entropy conservation.** *The fluxes for the phasic entropies $\alpha_k \rho_k s_k$ are conservative: $\mathbf{F}_i^-(\mathbb{U}_L, \mathbb{U}_R) = \mathbf{F}_i^+(\mathbb{U}_L, \mathbb{U}_R)$ for i in $\{6, 7\}$. Hence, denoting $(\alpha_k \rho_k s_k u_k)_{j+\frac{1}{2}}^n = \mathbf{F}_{5+k}^\pm(\mathbb{U}_j^n, \mathbb{U}_{j+1}^n)$ for $k = 1, 2$, one has:*

$$(\alpha_k \rho_k s_k)_j^{n+1} = (\alpha_k \rho_k s_k)_j^n - \frac{\Delta t}{\Delta x} \left((\alpha_k \rho_k s_k u_k)_{j+\frac{1}{2}}^n - (\alpha_k \rho_k s_k u_k)_{j-\frac{1}{2}}^n \right). \quad (60)$$

- **Total momentum conservation.** *The fluxes for the mixture momentum $\sum_{k=1,2} \alpha_k \rho_k u_k$ are conservative: $\sum_{k=1,2} \mathbf{F}_{3+k}^-(\mathbb{U}_L, \mathbb{U}_R) = \sum_{k=1,2} \mathbf{F}_{3+k}^+(\mathbb{U}_L, \mathbb{U}_R)$. Hence, denoting $(\sum_{k=1,2} \alpha_k \rho_k u_k^2 + \alpha_k \pi_k)_{j+\frac{1}{2}}^n = \sum_{k=1,2} \mathbf{F}_{3+k}^\pm(\mathbb{U}_j^n, \mathbb{U}_{j+1}^n)$ for $k = 1, 2$, one has:*

$$\begin{aligned} \sum_{k=1}^2 (\alpha_k \rho_k u_k)_j^{n+1} &= \sum_{k=1}^2 (\alpha_k \rho_k u_k)_j^n - \frac{\Delta t}{\Delta x} \left(\sum_{k=1,2} \alpha_k \rho_k u_k^2 + \alpha_k \pi_k \right)_{j+\frac{1}{2}}^n \\ &+ \frac{\Delta t}{\Delta x} \left(\sum_{k=1,2} \alpha_k \rho_k u_k^2 + \alpha_k \pi_k \right)_{j-\frac{1}{2}}^n. \end{aligned} \quad (61)$$

- **Discrete energy inequalities.** *Assume that the relaxation parameters $(a_k)_{j+\frac{1}{2}}^n$, $k = 1, 2$ satisfy Whitham's condition at each time step and each interface, i.e. that for all $n \in \mathbb{N}$, $j \in \mathbb{Z}$, $(a_k)_{j+\frac{1}{2}}^n$, $k = 1, 2$ are large enough so that*

$$((a_k)_{j+\frac{1}{2}}^n)^2 > -\partial_{\tau_k} \mathcal{P}_k(\mathcal{T}_k, s_k), \quad (62)$$

for all \mathcal{T}_k and s_k in the solution $\xi \mapsto \mathbb{W}_r(\xi; \mathcal{M}(\mathbb{U}_j^n), \mathcal{M}(\mathbb{U}_{j+1}^n))$. Then, the values \mathbb{U}_j^n , $j \in \mathbb{Z}$, $n \in \mathbb{N}$, computed by the scheme satisfy the following discrete energy inequalities:

$$\begin{aligned}
(\alpha_k \rho_k E_k)(\mathbb{U}_j^{n+1}) \leq (\alpha_k \rho_k E_k)(\mathbb{U}_j^n) & - \frac{\Delta t}{\Delta x} \left((\alpha_k \rho_k \mathcal{E}_k u_k + \alpha_k \pi_k u_k)_{j+\frac{1}{2}}^n - (\alpha_k \rho_k \mathcal{E}_k u_k + \alpha_k \pi_k u_k)_{j-\frac{1}{2}}^n \right) \\
& + \frac{\Delta t}{\Delta x} \mathbb{1}_{\{(u_2^*)_{j-\frac{1}{2}}^n \geq 0\}} (u_2^* \pi_1^*)_{j-\frac{1}{2}}^n \left((\alpha_k)_j^n - (\alpha_k)_{j-1}^n \right) \\
& + \frac{\Delta t}{\Delta x} \mathbb{1}_{\{(u_2^*)_{j+\frac{1}{2}}^n \leq 0\}} (u_2^* \pi_1^*)_{j+\frac{1}{2}}^n \left((\alpha_k)_{j+1}^n - (\alpha_k)_j^n \right),
\end{aligned} \tag{63}$$

where for $j \in \mathbb{Z}$, $(\alpha_k \rho_k \mathcal{E}_k u_k + \alpha_k \pi_k u_k)_{j+\frac{1}{2}}^n = (\alpha_k \rho_k \mathcal{E}_k u_k + \alpha_k \pi_k u_k)(\mathbb{W}_r(0^+; \mathcal{M}(\mathbb{U}_j^n), \mathcal{M}(\mathbb{U}_{j+1}^n)))$ is the right hand side trace of the phasic energy flux evaluated at $x_{j+\frac{1}{2}}$.

Note that (59) and (60) are updating formulae for the next time step unknown \mathbb{U}_j^{n+1} whereas (61) and the energy inequalities (63) are properties satisfied by the values \mathbb{U}_j^n , $j \in \mathbb{Z}$, $n \in \mathbb{N}$, computed by the numerical scheme.

Proof of Prop. 3.7. The approximate Riemann solver is a Godunov type scheme where \mathbb{U}_j^{n+1} is the cell-average over C_j of the function $\mathbb{U}_{app}(x, t)$. Hence, the positivity property is a direct consequence of Theorem 3.5 which ensures the positivity of the phase fractions and entropies (which are simply transported) and of the densities in the relaxation Riemann solver. For this purpose, energy dissipation (41) across the u_2 -contact discontinuity may be necessary for enforcing this property when the ratio $\frac{\alpha_{1,j}}{\alpha_{1,j+1}}$ (or its inverse) is large for some $j \in \mathbb{Z}$.

The proof of (59), (60) and (61) involves no particular difficulties. It is a direct consequence of equations (36), (37) and (38) satisfied by the relaxation Riemann solutions at each interface.

Let us prove the discrete energy inequalities (63) satisfied by the scheme under Whitham's condition (62). Assuming the CFL condition (55), the solution of (24) over $[x_{j-\frac{1}{2}}, x_{j+\frac{1}{2}}] \times [t^n, t^{n+1}]$ is the function

$$\begin{aligned}
\mathbb{W}(x, t) := \mathbb{W}_r \left(\frac{x - x_{j-\frac{1}{2}}}{t - t^n}; \mathcal{M}(\mathbb{U}_{j-1}^n), \mathcal{M}(\mathbb{U}_j^n) \right) \mathbb{1}_{[x_{j-\frac{1}{2}}, x_j]}(x) \\
+ \mathbb{W}_r \left(\frac{x - x_{j+\frac{1}{2}}}{t - t^n}; \mathcal{M}(\mathbb{U}_j^n), \mathcal{M}(\mathbb{U}_{j+1}^n) \right) \mathbb{1}_{[x_j, x_{j+\frac{1}{2}}]}(x).
\end{aligned} \tag{64}$$

According to Theorem 3.5, this function satisfies the phase 1 energy equation:

$$\begin{aligned}
\partial_t(\alpha_1 \rho_1 \mathcal{E}_1) + \partial_x(\alpha_1 \rho_1 \mathcal{E}_1 u_1 + \alpha_1 \pi_1 u_1) - u_2^* \pi_1^* \partial_x \alpha_1 = \\
- \mathcal{Q}_{j-\frac{1}{2}}^n \delta_0 \left(x - x_{j-\frac{1}{2}} - (u_2^*)_{j-\frac{1}{2}}^n (t - t^n) \right) - \mathcal{Q}_{j+\frac{1}{2}}^n \delta_0 \left(x - x_{j+\frac{1}{2}} - (u_2^*)_{j+\frac{1}{2}}^n (t - t^n) \right),
\end{aligned} \tag{65}$$

where for $i \in \mathbb{Z}$, we have denoted $\mathcal{Q}_{i-\frac{1}{2}}^n = \mathcal{Q} \left((u_2^*)_{i-\frac{1}{2}}^n, \mathcal{M}(\mathbb{U}_{i-1}^n), \mathcal{M}(\mathbb{U}_i^n) \right)$. Integrating this equation over $]x_{j-\frac{1}{2}}, x_{j+\frac{1}{2}}[\times [t^n, t^{n+1}]$ and dividing by Δx yields:

$$\begin{aligned}
\frac{1}{\Delta x} \int_{x_{j-\frac{1}{2}}}^{x_{j+\frac{1}{2}}} (\alpha_1 \rho_1 \mathcal{E}_1)(\mathbb{W}(x, t^{n+1})) dx & \leq (\alpha_1 \rho_1 \mathcal{E}_1)(\mathcal{M}(\mathbb{U}_j^n)) \\
& - \frac{\Delta t}{\Delta x} (\alpha_1 \rho_1 \mathcal{E}_1 u_1 + \alpha_1 \pi_1 u_1) (\mathbb{W}_r(0^-; \mathcal{M}(\mathbb{U}_j^n), \mathcal{M}(\mathbb{U}_{j+1}^n))) \\
& + \frac{\Delta t}{\Delta x} (\alpha_1 \rho_1 \mathcal{E}_1 u_1 + \alpha_1 \pi_1 u_1) (\mathbb{W}_r(0^+; \mathcal{M}(\mathbb{U}_{j-1}^n), \mathcal{M}(\mathbb{U}_j^n))) \\
& + \frac{\Delta t}{\Delta x} \mathbb{1}_{\{(u_2^*)_{j-\frac{1}{2}}^n \geq 0\}} (u_2^* \pi_1^*)_{j-\frac{1}{2}}^n \left((\alpha_1)_j^n - (\alpha_1)_{j-1}^n \right) \\
& + \frac{\Delta t}{\Delta x} \mathbb{1}_{\{(u_2^*)_{j+\frac{1}{2}}^n \leq 0\}} (u_2^* \pi_1^*)_{j+\frac{1}{2}}^n \left((\alpha_1)_{j+1}^n - (\alpha_1)_j^n \right),
\end{aligned} \tag{66}$$

because $\mathcal{Q}_{j-\frac{1}{2}}^n \geq 0$ and $\mathcal{Q}_{j+\frac{1}{2}}^n \geq 0$. Since the initial data is at equilibrium: $\mathbb{W}(x, t^n) = \mathcal{M}(\mathbb{U}_j^n)$ for all $x \in C_j$ (*i.e.* $(\mathcal{T}_1)_j^n$ is set to be equal to $(\tau_1)_j^n$) one has $(\alpha_1 \rho_1 \mathcal{E}_1)(\mathcal{M}(\mathbb{U}_j^n)) = (\alpha_1 \rho_1 E_1)(\mathbb{U}_j^n)$ according to Proposition 3.2. Applying the Rankine-Hugoniot jump relation to (65) across the line $\{(x, t), x = x_{j+\frac{1}{2}}, t > 0\}$, yields:

$$\begin{aligned} & (\alpha_1 \rho_1 \mathcal{E}_1 u_1 + \alpha_1 \pi_1 u_1) (\mathbb{W}_r(0^-; \mathcal{M}(\mathbb{U}_j^n), \mathcal{M}(\mathbb{U}_{j+1}^n))) \\ &= (\alpha_1 \rho_1 \mathcal{E}_1 u_1 + \alpha_1 \pi_1 u_1) (\mathbb{W}_r(0^+; \mathcal{M}(\mathbb{U}_j^n), \mathcal{M}(\mathbb{U}_{j+1}^n))) + \mathcal{Q}_{j+\frac{1}{2}}^n \mathbb{1}_{\{(u_2^*)_{j+\frac{1}{2}}^n = 0\}}. \end{aligned}$$

Hence, since $\mathcal{Q}_{j+\frac{1}{2}}^n \geq 0$, for the interface $x_{j+\frac{1}{2}}$, taking the trace of $(\alpha_1 \rho_1 \mathcal{E}_1 u_1 + \alpha_1 \pi_1 u_1)$ at 0^+ instead of 0^- in (66) only improves the inequality. Furthermore, assuming that the parameter a_1 satisfies Whitham's condition (62), the Gibbs principle stated in (23) holds true so that:

$$\frac{1}{\Delta x} \int_{x_{j-\frac{1}{2}}}^{x_{j+\frac{1}{2}}} (\alpha_1 \rho_1 E_1)(\mathbb{U}_{app}(x, t^{n+1})) dx \leq \frac{1}{\Delta x} \int_{x_{j-\frac{1}{2}}}^{x_{j+\frac{1}{2}}} (\alpha_1 \rho_1 \mathcal{E}_1)(\mathbb{W}(x, t^{n+1})) dx.$$

Invoking the convexity of the mapping $\mathbb{U} \mapsto (\alpha_1 \rho_1 E_1)(\mathbb{U})$ (see Prop. 3.1), Jensen's inequality implies that

$$(\alpha_1 \rho_1 E_1)(\mathbb{U}_j^{n+1}) \leq \frac{1}{\Delta x} \int_{x_{j-\frac{1}{2}}}^{x_{j+\frac{1}{2}}} (\alpha_1 \rho_1 E_1)(\mathbb{U}_{app}(x, t^{n+1})) dx,$$

which yields the desired discrete energy inequality for phase 1. The proof of the discrete energy inequality for phase 2 follows similar steps. \square

4 A positive and entropy-satisfying scheme for the Baer-Nunziato model

In the previous section we have designed a numerical scheme for an auxiliary two-phase flow model where the exact solutions conserve the phasic entropies while the phasic energies are dissipated by shock solutions. The scheme has been proven to satisfy discrete counterparts of these features while ensuring the positivity of the relevant quantities.

In the present section, we describe the correction to be given to the auxiliary scheme in order to conserve the phasic energies while dissipating the phasic entropies. We end up with a numerical scheme which is consistent with the entropy weak solutions of any Cauchy problem associated with the original Baer-Nunziato model (1):

$$\begin{cases} \partial_t \mathcal{U} + \partial_x \mathcal{F}(\mathcal{U}) + \mathcal{C}(\mathcal{U}) \partial_x \mathcal{U} = 0, & x \in \mathbb{R}, t > 0, \\ \mathcal{U}(x, 0) = \mathcal{U}_0(x), & x \in \mathbb{R}. \end{cases} \quad (67)$$

We keep the same time and space discretization as described in Section 3.3. The approximate solution at time t^n , $x \in \mathbb{R} \mapsto \mathcal{U}_\lambda(x, t^n) \in \Omega$ is a piecewise constant function whose value on each cell C_j is a constant value denoted by \mathcal{U}_j^n . The updated value \mathcal{U}_j^{n+1} is computed through a two-step algorithm described hereunder:

4.1 A fractional step algorithm

• **Step 1: updating the auxiliary unknown.** Given

$$\mathcal{U}_j^n = ((\alpha_1)_j^n, (\alpha_1 \rho_1)_j^n, (\alpha_2 \rho_2)_j^n, (\alpha_1 \rho_1 u_1)_j^n, (\alpha_2 \rho_2 u_2)_j^n, (\alpha_1 \rho_1 E_1)_j^n, (\alpha_2 \rho_2 E_2)_j^n)^T,$$

we begin with setting the auxiliary unknown \mathbb{U}_j^n as follows:

$$\mathbb{U}_j^n = ((\alpha_1)_j^n, (\alpha_1 \rho_1)_j^n, (\alpha_2 \rho_2)_j^n, (\alpha_1 \rho_1 u_1)_j^n, (\alpha_2 \rho_2 u_2)_j^n, (\alpha_1 \rho_1 s_1)(\mathcal{U}_j^n), (\alpha_2 \rho_2 s_2)(\mathcal{U}_j^n))^T,$$

where $(\alpha_k \rho_k s_k)(\mathcal{U}_j^n)$ is the partial entropy of phase k , computed from \mathcal{U}_j^n , knowing the total energy E_k and the kinetic energy $u_k^2/2$. Observe that, with this definition of \mathbb{U}_j^n , one has $(\alpha_k \rho_k E_k)(\mathbb{U}_j^n) = (\alpha_k \rho_k E_k)_j^n$.

We then compute $\mathbb{U}_j^{n+1,-}$ by applying the relaxation scheme designed for the auxiliary model:

$$\mathbb{U}_j^{n+1,-} = \mathbb{U}_j^n - \frac{\Delta t}{\Delta x} (\mathbf{F}^-(\mathbb{U}_j^n, \mathbb{U}_{j+1}^n) - \mathbf{F}^+(\mathbb{U}_{j-1}^n, \mathbb{U}_j^n)). \quad (68)$$

According to Proposition 3.7 the phasic energies are dissipated at the discrete level following:

$$\begin{aligned} (\alpha_k \rho_k E_k)(\mathbb{U}_j^{n+1,-}) &\leq (\alpha_k \rho_k E_k)_j^n - \frac{\Delta t}{\Delta x} \left((\alpha_k \rho_k \mathcal{E}_k u_k + \alpha_k \pi_k u_k)_{j+\frac{1}{2}}^n - (\alpha_k \rho_k \mathcal{E}_k u_k + \alpha_k \pi_k u_k)_{j-\frac{1}{2}}^n \right) \\ &\quad + \frac{\Delta t}{\Delta x} \mathbb{1}_{\{(u_2^*)_{j-\frac{1}{2}}^n \geq 0\}} (u_2^* \pi_1^*)_{j-\frac{1}{2}}^n ((\alpha_k)_j^n - (\alpha_k)_{j-1}^n) \\ &\quad + \frac{\Delta t}{\Delta x} \mathbb{1}_{\{(u_2^*)_{j+\frac{1}{2}}^n \leq 0\}} (u_2^* \pi_1^*)_{j+\frac{1}{2}}^n ((\alpha_k)_{j+1}^n - (\alpha_k)_j^n). \end{aligned} \quad (69)$$

• **Step 2: Exchanging energy and entropy.** This final step is a correction step which aims at enforcing conservative updates for the energies of the original unknown \mathcal{U}_j^{n+1} . It simply consists in keeping unchanged the updates of the phase fractions, partial masses and momentum:

$$(\alpha_1)_j^{n+1} := (\alpha_1)_j^{n+1,-}, \quad (\alpha_k \rho_k)_j^{n+1} := (\alpha_k \rho_k)_j^{n+1,-}, \quad (\alpha_k \rho_k u_k)_j^{n+1} := (\alpha_k \rho_k u_k)_j^{n+1,-}, \quad k = 1, 2, \quad (70)$$

while enforcing energy conservation by defining the energies updates as:

$$\begin{aligned} (\alpha_k \rho_k E_k)_j^{n+1} &:= (\alpha_k \rho_k E_k)_j^n - \frac{\Delta t}{\Delta x} \left((\alpha_k \rho_k \mathcal{E}_k u_k + \alpha_k \pi_k u_k)_{j+\frac{1}{2}}^n - (\alpha_k \rho_k \mathcal{E}_k u_k + \alpha_k \pi_k u_k)_{j-\frac{1}{2}}^n \right) \\ &\quad + \frac{\Delta t}{\Delta x} \mathbb{1}_{\{(u_2^*)_{j-\frac{1}{2}}^n \geq 0\}} (u_2^* \pi_1^*)_{j-\frac{1}{2}}^n ((\alpha_k)_j^n - (\alpha_k)_{j-1}^n) \\ &\quad + \frac{\Delta t}{\Delta x} \mathbb{1}_{\{(u_2^*)_{j+\frac{1}{2}}^n \leq 0\}} (u_2^* \pi_1^*)_{j+\frac{1}{2}}^n ((\alpha_k)_{j+1}^n - (\alpha_k)_j^n). \end{aligned} \quad (71)$$

4.2 Finite volume formulation of the scheme

In practice, in the implementation, when performing the first step of the method, *i.e.* when applying the relaxation scheme to the auxiliary variable \mathbb{U} , one does not update the last two variables which are the phasic entropies. Indeed, computing the phasic entropies $(\alpha_k \rho_k s_k)_j^{n+1,-}$ is not needed for the update of the phasic energies which is performed in the second step. Therefore, the two step algorithm described in the previous section can be reformulated as a classical non-conservative finite volume scheme. Indeed, we have the following result:

Proposition 4.1. *The two step algorithm described in equations (68)-(70)-(71) is equivalent to the following non-conservative finite volume scheme:*

$$\mathcal{U}_j^{n+1} = \mathcal{U}_j^n - \frac{\Delta t}{\Delta x} (\mathcal{F}^-(\mathcal{U}_j^n, \mathcal{U}_{j+1}^n) - \mathcal{F}^+(\mathcal{U}_{j-1}^n, \mathcal{U}_j^n)). \quad (72)$$

where the first five components of $\mathcal{F}^\pm(\mathcal{U}_L, \mathcal{U}_R)$ coincide with the first five components of $\mathbf{F}^\pm(\mathbb{U}_L, \mathbb{U}_R)$ with \mathbb{U} computed from \mathcal{U} by imposing $\alpha_k \rho_k s_k = (\alpha_k \rho_k s_k)(\mathcal{U})$. The last two components of $\mathcal{F}^\pm(\mathcal{U}_L, \mathcal{U}_R)$ are given for $k \in \{1, 2\}$ by:

$$\begin{aligned} \mathcal{F}_{5+k}^-(\mathcal{U}_L, \mathcal{U}_R) &= (\alpha_k \rho_k \mathcal{E}_k u_k + \alpha_k \pi_k u_k) (\mathbb{W}_r(0^+; \mathcal{M}(\mathbb{U}_L), \mathcal{M}(\mathbb{U}_R))) + \mathbb{1}_{\{u_2^* \leq 0\}} (u_2^* \pi_1^*) ((\alpha_k)_R - (\alpha_k)_L), \\ \mathcal{F}_{5+k}^+(\mathcal{U}_L, \mathcal{U}_R) &= (\alpha_k \rho_k \mathcal{E}_k u_k + \alpha_k \pi_k u_k) (\mathbb{W}_r(0^+; \mathcal{M}(\mathbb{U}_L), \mathcal{M}(\mathbb{U}_R))) - \mathbb{1}_{\{u_2^* \geq 0\}} (u_2^* \pi_1^*) ((\alpha_k)_R - (\alpha_k)_L). \end{aligned}$$

Proof. The proposition follows from elementary verifications using equations (68)-(70)-(71) and the expressions of the energy numerical fluxes $(\alpha_k \rho_k \mathcal{E}_k u_k + \alpha_k \pi_k u_k)_{j+\frac{1}{2}}$ given in Proposition 3.7. \square

For the reader who is eager to rapidly implement the numerical scheme, we refer to appendix 7.2 where the expressions of the numerical fluxes $\mathcal{F}^\pm(\mathcal{U}_L, \mathcal{U}_R)$ are given in detail.

Recasting the scheme in a finite volume formulation with two interface fluxes $\mathcal{F}^\pm(\mathcal{U}_L, \mathcal{U}_R)$ is very interesting since it allows a nearly straightforward extension of the scheme to the 2D and 3D versions of the Baer-Nunziato model on unstructured meshes. Indeed, the multi-dimensional Baer-Nunziato model is invariant by Galilean transformations. Therefore, by assuming that, in the neighborhood of a multi-D cell interface, one has a local 1D Riemann problem in the orthogonal direction to the interface, it is possible to use the very same fluxes $\mathcal{F}^\pm(\mathcal{U}_L, \mathcal{U}_R)$.

4.3 Main properties of the scheme

We may now state the following theorem, which gathers the main properties of this scheme, and which constitutes the main result of the paper.

Theorem 4.2. *The finite volume scheme (72) for the Baer-Nunziato model has the following properties:*

- **Positivity:** *Under the CFL condition (55), it preserves positive values of the phase fractions, densities and internal energies: for all $n \in \mathbb{N}$, if $(\mathcal{U}_j^n \in \Omega_{\mathcal{U}})$ for all $j \in \mathbb{Z}$, then $0 < (\alpha_k)_j^{n+1} < 1$, $(\alpha_k \rho_k)_j^{n+1} > 0$, and $(E_k - u_k^2/2)_j^{n+1} > 0$ for $k = 1, 2$ and all $j \in \mathbb{Z}$, i.e. $(\mathcal{U}_j^{n+1} \in \Omega_{\mathcal{U}})$ for all $j \in \mathbb{Z}$.*
- **Conservativity:** *The discretization of the partial masses $\alpha_k \rho_k$, $k \in \{1, 2\}$, the total mixture momentum $\alpha_1 \rho_1 u_1 + \alpha_2 \rho_2 u_2$ and the total mixture energy $\alpha_1 \rho_1 E_1 + \alpha_2 \rho_2 E_2$, is conservative.*
- **Discrete entropy inequalities.** *Assume that the relaxation parameters $(a_k)_{j+\frac{1}{2}}^n$, $k = 1, 2$ satisfy Whitham's condition at each time step and each interface, i.e. that for all $n \in \mathbb{N}$, $j \in \mathbb{Z}$, $(a_k)_{j+\frac{1}{2}}^n$, $k = 1, 2$ are large enough so that*

$$((a_k)_{j+\frac{1}{2}}^n)^2 > -\partial_{\tau_k} \mathcal{P}_k(\mathcal{T}_k, s_k), \quad (73)$$

for all \mathcal{T}_k and s_k in the solution $\xi \mapsto \mathbb{W}_r(\xi; \mathcal{M}(\mathbb{U}_j^n), \mathcal{M}(\mathbb{U}_{j+1}^n))$. Then, the values \mathcal{U}_j^n computed by the scheme satisfy the following discrete entropy inequalities: for $k = 1, 2$:

$$(\alpha_k \rho_k s_k)(\mathcal{U}_j^{n+1}) \leq (\alpha_k \rho_k s_k)(\mathcal{U}_j^n) - \frac{\Delta t}{\Delta x} \left((\alpha_k \rho_k s_k u_k)_{j+\frac{1}{2}}^n - (\alpha_k \rho_k s_k u_k)_{j-\frac{1}{2}}^n \right), \quad (74)$$

where the entropy fluxes $(\alpha_k \rho_k s_k u_k)_{j+\frac{1}{2}}^n$ are defined in Proposition 3.7. These inequalities are discrete counterparts of the entropy inequalities (9) satisfied by the admissible weak solutions of the Baer-Nunziato model (1).

Note that preserving positive values of the phase fractions, the phasic densities and also the phasic internal energies altogether is an unprecedented result. Furthermore, up to our knowledge, this scheme is the first scheme approximating the solutions of the Baer-Nunziato model, for which discrete entropy inequalities (9) are proven.

Proof. The positivity of the phase fractions $(\alpha_k)_j^{n+1}$ and partial masses $(\alpha_k \rho_k)_j^{n+1}$ follows directly from Proposition 3.7. To check that the proposed algorithm preserves the positivity of the internal energies, namely $(e_k)_j^{n+1} = (E_k - u_k^2/2)_j^{n+1} > 0$, it suffices to notice that before the update of the energy in the second step, the update $(s_k)_j^{n+1,-}$, computed by the relaxation scheme in the first step, obeys a discrete local maximum principle so that $(e_k)_j^{n+1,-} := e_k((\tau_k)_j^{n+1,-}, (s_k)_j^{n+1,-})$ is well defined and thus positive provided that $(\alpha_k \rho_k)_j^{n+1,-} > 0$, which is true. The second step results in increasing the total

energies and one has $(\alpha_k \rho_k E_k)_j^{n+1} \geq (\alpha_k \rho_k E_k)(\mathbb{U}_j^{n+1,-})$ by (69)-(71), while $(\alpha_k \rho_k)_j^{n+1} = (\alpha_k \rho_k)_j^{n+1,-}$, which yields $(E_k)_j^{n+1} \geq E_k(\mathbb{U}_j^{n+1,-})$. Now, as the kinetic energy $((u_k)_j^{n+1,-})^2/2$ is unchanged by the second step and $E_k(\mathbb{U}_j^{n+1,-}) = (e_k)_j^{n+1,-} - ((u_k)_j^{n+1,-})^2/2$, we infer that $(e_k)_j^{n+1} \geq (e_k)_j^{n+1,-} > 0$ and hence the required positivity property for the internal energies.

We now prove the discrete entropy inequalities (74). The first step provides a conservative update of the phasic entropy equations. Indeed, the last two components of the vector equation (68) yield

$$(\alpha_k \rho_k s_k)_j^{n+1,-} = (\alpha_k \rho_k s_k)(\mathcal{U}_j^n) - \frac{\Delta t}{\Delta x} \left((\alpha_k \rho_k s_k u_k)_{j+\frac{1}{2}}^n - (\alpha_k \rho_k s_k u_k)_{j-\frac{1}{2}}^n \right). \quad (75)$$

Then, thanks to the thermodynamics assumptions, we know from Proposition 3.1 that

$$\partial_{\alpha_k \rho_k E_k}(\alpha_k \rho_k s_k)(\mathcal{U}) = -1/T_k.$$

Consequently, we infer from $(\alpha_k \rho_k E_k)_j^{n+1} \geq (\alpha_k \rho_k E_k)(\mathbb{U}_j^{n+1,-})$ that $(\alpha_k \rho_k s_k)(\mathcal{U}_j^{n+1}) \leq (\alpha_k \rho_k s_k)_j^{n+1,-}$. Injecting in (75) yields the discrete entropy inequalities (74). \square

For most equations of state, that are given as a function $p_k(\rho_k, e_k)$, the quantity $\alpha_k \rho_k s_k$ cannot be expressed as an explicit function of \mathcal{U} , which makes it even impossible to compute the time step initial values of the entropies $(\alpha_k \rho_k s_k)(\mathcal{U}_j^n)$. Still, this does not prevent the discrete inequalities (74) to hold true.

The impossibility, for many equations of state, to express the entropies s_k explicitly does not prevent the computation of the numerical fluxes $\mathcal{F}_i^\pm(\mathcal{U}_j^n, \mathcal{U}_{j+1}^n)$, $i = 1, \dots, 7$, for the updates of $(\alpha_1)_j^{n+1}$, $(\alpha_k \rho_k)_j^{n+1}$, $(\alpha_k \rho_k u_k)_j^{n+1}$ in the first step, and the updates of $(\alpha_k \rho_k E_k)_j^{n+1}$ in the second step. Indeed, even though these numerical fluxes involve terms of the form $e_k(\mathcal{T}_k, s_k)$ and $\pi_k(\tau_k, \mathcal{T}_k, s_k)$ to be evaluated on the relaxation Riemann solution of the first step, the discussion of Section 3.2 shows that these functions are solely evaluated on the piecewise constant initial data in terms of $e_k((\mathcal{T}_k)_j^n, (s_k)_j^n)$ and $\mathcal{P}_k((\mathcal{T}_k)_j^n, (s_k)_j^n)$. But observe that by the thermodynamics, $e_k((\mathcal{T}_k)_j^n, (s_k)_j^n)$ is nothing else but $(e_k)_j^n = (E_k)_j^n - ((u_k)_j^n)^2/2$ and $\mathcal{P}_k((\mathcal{T}_k)_j^n, (s_k)_j^n)$ is equal to $p_k((\rho_k)_j^n, (e_k)_j^n)$. Hence, even though the entropy is used for the analysis of the numerical method, one may implement this scheme even for general and possibly incomplete equations of state that are given as a function $p_k(\rho_k, e_k)$, since the numerical fluxes may still be computed at each time step in terms of the initial unknowns $\mathcal{U}_j^n, j \in \mathbb{Z}$.

5 Numerical tests

In this section, we present Riemann-type test-cases on which the performances of the relaxation scheme are tested. The thermodynamics follow either an ideal gas or a stiffened gas law:

$$p_k(\rho_k, e_k) = (\gamma_k - 1)\rho_k e_k - \gamma_k p_{\infty, k},$$

where $\gamma_k > 1$ and $p_{\infty, k} \geq 0$ are two constants. The e.o.s. parameters of each test-case are given in Table 1 as well as the initial discontinuity position, the final time and the CFL number. The initial and intermediate states of each solution are displayed in Tables 2 to 6. The u_2 -contact discontinuity separates two regions denoted $-$ and $+$ respectively on the left and right sides of the discontinuity. If the u_1 -contact discontinuity has non-zero strength, an additional region L^* or R^* also exists according to the sign of $u_2 - u_1$ as described in Figure 1.

We recall that the scheme relies on a relaxation Riemann solver which requires solving a fixed point in order to compute, for every cell interface $x_{j+\frac{1}{2}}$, the zero of a scalar function (see eq. (79) in Appendix 7.2). A dichotomy method is used in order to compute this solution. The iterative procedure is stopped when the error is less than 10^{-12} .

	Test 1	Test 2	Test 3	Test 4	Test 5
γ_1	1.4	1.4	1.4	3	3
$p_{\infty,1}$	0	0	0	0	0
γ_2	1.4	3	1.4	1.4	1.4
$p_{\infty,2}$	0	100	0	0	0
x_0	0	0.8	0.5	0	0
T_{\max}	0.15	0.007	0.15	0.15	0.05
CFL	0.45	0.45	0.45	0.45	0.45

Table 1: E.O.S. parameters, initial discontinuity position, final time, Courant-Friedrichs-Lewy number.

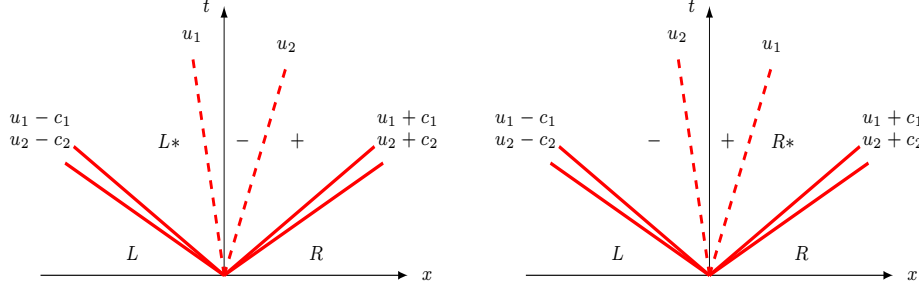


Figure 1: Structure of the Riemann solutions, notations for the intermediate states.

	Region L	Region L^*	Region $-$	Region $+$	Region R
α_1	0.2	0.2	0.2	0.7	0.7
ρ_1	0.21430	0.35	0.698	0.90583	0.96964
u_1	-0.02609	-0.7683	-0.7683	-0.11581	-0.03629
p_1	0.3	0.6045	0.6045	0.87069	0.95776
ρ_2	1.00003	1.00003	0.9436	1.0591	0.99993
u_2	0.00007	0.00007	0.0684	0.0684	-0.00004
p_2	1.0	0.9219	0.9219	1.08383	1.0

Table 2: Test-case 1: Left, right and intermediate states of the exact solution.

5.1 Results for Test-case 1

In this first test-case, both phases follow an ideal gas e.o.s. (see Table 1). The wave pattern for phase 1 consists of a left-traveling shock, a material contact discontinuity u_1 , a phase fraction discontinuity of velocity u_2 and a right-traveling rarefaction wave. For phase 2 the wave pattern is composed of a left-traveling rarefaction wave, the phase fraction discontinuity, and a right-traveling shock.

In Figure 2, the approximate solution computed with the relaxation scheme is compared with both the exact solution and the approximate solution obtained with Rusanov's scheme (a Lax-Friedrichs type scheme, see [23]). The results show that unlike Rusanov's scheme, the relaxation method correctly captures the intermediate states even for this rather coarse mesh of 100 cells. This coarse mesh is a typical example of an industrial mesh, reduced to one direction, since 100 cells in 1D correspond to a 10^6 -cell mesh in 3D. It appears that the contact discontinuity is captured more sharply by the relaxation method than by Rusanov's scheme for which the numerical diffusion is larger. We can also see that for the phase 2 variables, there are no oscillations as one can see for Rusanov's scheme: the curves are monotone between the intermediate states. As for phase 1, the intermediate states are captured by the relaxation method while with Rusanov's scheme, this weak level of refinement is clearly not enough to capture any intermediate state. These observations assess that, for the same

level of refinement, the relaxation method is much more accurate than Rusanov’s scheme.

A mesh refinement process has also been implemented in order to check numerically the convergence of the method, as well as its performances in terms of CPU-time cost. For this purpose, we compute the discrete L^1 -error between the approximate solution and the exact one at the final time $T_{\max} = N\Delta t$, normalized by the discrete L^1 -norm of the exact solution:

$$E(\Delta x) = \frac{\sum_j |\phi_j^N - \phi_{ex}(x_j, T_{\max})| \Delta x}{\sum_j |\phi_{ex}(x_j, T)| \Delta x}, \quad (76)$$

where ϕ is any of the non conservative variables $(\alpha_1, \rho_1, u_1, p_1, \rho_2, u_2, p_2)$. The calculations have been implemented on several meshes composed of 100×2^n cells with $n = 0, 1, \dots, 10$ (knowing that the domain size is $L = 1$). In Figure 3, the error $E(\Delta x)$ at the final time $T_{\max} = 0.15$, is plotted against Δx in a $\log - \log$ scale. We can see that all the errors converge towards zero with the expected order of $\Delta x^{1/2}$, except the error for u_2 which seems to converge with a higher rate. However, $\Delta x^{1/2}$ is only an asymptotic order of convergence, and in this particular case, one would have to implement the calculation on more refined meshes in order to reach the theoretically expected order of $\Delta x^{1/2}$.

Figure 3 also displays the error on the non conservative variables with respect to the CPU-time of the calculation expressed in seconds. Each point of the plot corresponds to one single calculation for a given mesh size. One can see that, if one prescribes a given level of the error, the computational cost of Rusanov’s scheme is significantly higher than that of the relaxation method for all the variables. For instance, for the same error on the phase 1 density ρ_1 , the gain in computational cost is more than a hundred times when using the relaxation method rather than Rusanov’s scheme!

5.2 Results for Test-case 2

	Region L	Region $-$	Region $+$	Region R^*	Region R
α_1	0.3	0.3	0.8	0.8	0.8
ρ_1	1.0	0.4684	0.50297	5.9991	1.0
u_1	-19.59741	6.7332	-1.75405	-1.75405	-19.59741
p_1	1000.0	345.8279	382.08567	382.08567	0.01
ρ_2	1.0	0.7687	1.6087	1.6087	1.0
u_2	-19.59716	-6.3085	-6.3085	-6.3085	-19.59741
p_2	1000.0	399.5878	466.72591	466.72591	0.01

Table 3: Test-case 2: Left, right and intermediate states of the exact solution.

The second test-case was taken from [41]. Phase 1 follows an ideal gas e.o.s. while phase 2 follows a stiffened gas e.o.s. (see Table 1). From left to right, the solution for phase 1 consists of a left-traveling rarefaction wave, the phase fraction discontinuity, a material contact discontinuity u_1 , and a right-traveling shock. For phase 2 the wave pattern is composed of a left-traveling rarefaction wave, the phase fraction discontinuity, and a right-traveling shock.

As the jump of initial pressures is very large, **strong shocks** are generated in each phase. The distance between the right shock and contact waves is small in phase 1, which makes it difficult for both the relaxation and Rusanov’s scheme to capture the intermediate states. We observe however that the relaxation scheme remains more accurate than Rusanov’s scheme. For phase 2, Rusanov’s scheme fails to correctly capture the speed of the right-going shock due to the large difference between the pressures before and after the shock. On the contrary, the relaxation scheme captures the shock with the correct speed.

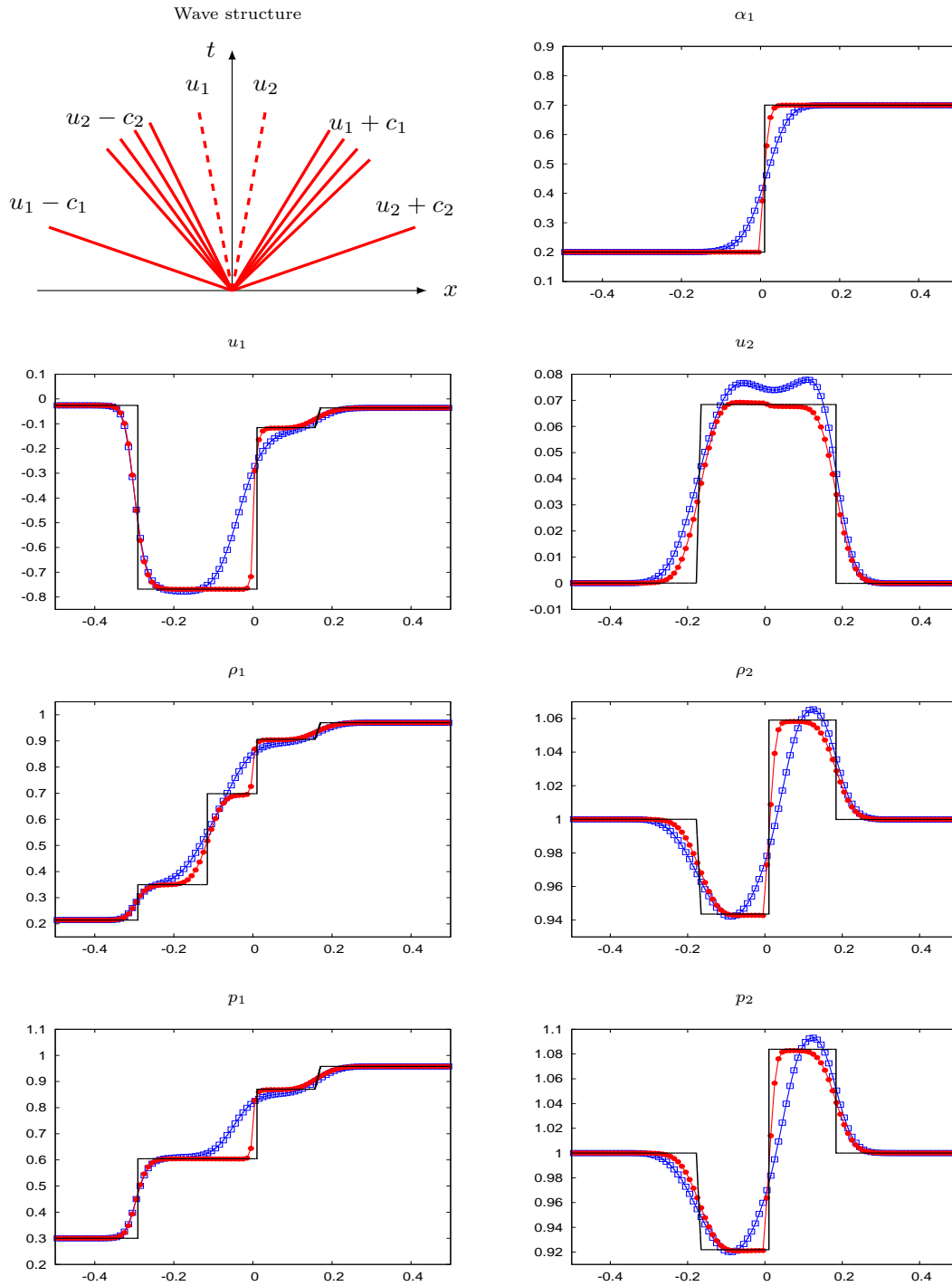


Figure 2: Test-case 1: Structure of the solution and space variations of the physical variables at the final time $T_{\max} = 0.15$. Mesh size: 100 cells. Straight line: exact solution, bullets: relaxation scheme, squares: Rusanov's scheme.

A convergence study has also been performed for this test-case. The observed convergence rate is slightly larger than $\Delta x^{1/2}$, and the error *v.s.* CPU plots show a smaller computational cost for the

relaxation scheme. However, on this test-case, the observed gain in the computational time is less than in the first test-case and is not the same for all the variables.

5.3 Results for Test-case 3

	Region L	Region $-$	Region $+$	Region R
α_1	0.2	0.2	0.5	0.5
ρ_1	0.99988	0.0219	0.0219	0.99988
u_1	-1.99931	0.0	0.0	1.99931
p_1	0.4	0.0019	0.0019	0.4
ρ_2	0.99988	0.0219	0.0219	0.99988
u_2	-1.99931	0.0	0.0	1.99931
p_2	0.4	0.0019	0.0019	0.4

Table 4: Test-case 3: Left, right and intermediate states of the exact solution.

This test was also taken from [41]. Both phases consist of two symmetric rarefaction waves and a stationary u_2 -contact discontinuity. As the region between the rarefaction waves is close to vacuum, this test-case is useful to assess the pressure positivity property. We can see that the computed pressures are positive for both schemes. In addition, both schemes have similar results, except for the resolution of the phase fraction discontinuity which appears to be very diffused by Rusanov’s scheme while it is **exactly captured** by the relaxation scheme, which is a property satisfied by the relaxation Riemann solver for this type of discontinuities.

5.4 Results for Test-case 4

	Region L	Region $-$	Region $+$	Region R^*	Region R
α_1	1.0	1.0	0.4	0.4	0.4
ρ_1	1.6	2.0	1.84850	2.03335	1.62668
u_1	0.80311	0.4	0.91147	0.91147	0.55623
p_1	1.3	2.6	2.05277	2.05277	1.02638
ρ_2	-	-	4.0	4.0	7.69667
u_2	-	-	0.1	0.1	0.74797
p_2	-	-	2.45335	2.45335	6.13338

Table 5: Test-case 4: Left, right and intermediate states of the exact solution.

We now consider a Riemann problem in which one of the two phases vanishes in one of the initial states, which means that the corresponding phase fraction α_1 or α_2 is equal to zero. For this kind of Riemann problem, the u_2 -contact separates a mixture region where the two phases coexist from a single phase region with the remaining phase. Various examples of such problems were introduced in [38], [37, 4] or [41].

The solution is composed of a $\{u_1 - c_1\}$ -shock wave in the left-hand side (LHS) region where only phase 1 is present. This region is separated by a u_2 -contact discontinuity from the right-hand side (RHS) region where the two phases are mixed. In this RHS region, the solution is composed of a u_1 -contact discontinuity, followed by a $\{u_2 + c_2\}$ -rarefaction wave and a $\{u_1 + c_1\}$ -shock (see Figure 7).

In practice, the numerical method requires values of $\alpha_{1,L}$ and $\alpha_{1,R}$ that lie strictly in the interval $(0, 1)$. Therefore, in the numerical implementation, we take $\alpha_{1,L} = 1 - 10^{-9}$. The aim here is to give a qualitative comparison between the numerical approximation and the exact solution. Moreover, there is theoretically no need to specify left initial values for the phase 2 quantities since this phase

is not present in the LHS region. For the sake of the numerical simulations however, one must provide such values. We choose to set $\rho_{2,L}$, $u_{2,L}$ and $p_{2,L}$ to the values on the right of the u_2 -contact discontinuity, which is coherent with the preservation of the Riemann invariants of this wave, and avoids the formation of fictitious acoustic waves for phase 2 in the LHS region. For the relaxation scheme, this choice enables to avoid oscillations of phase 2 quantities in the region where phase 2 is not present. However, some tests have been conducted that assess that taking other values of $(\rho_{2,L}, u_{2,L}, p_{2,L})$ has little impact on the phase 1 quantities as well as on the phase 2 quantities where this phase is present.

We can see that for the same level of refinement, the relaxation method is more accurate than Rusanov's scheme, which can be seen especially for phase 1. As regards the region where phase 2 does not exist, we can see that the relaxation method is much more stable than Rusanov's scheme. Indeed, the relaxation scheme behaves better than Rusanov's scheme when it comes to divisions by small values of α_2 , since the solution approximated by Rusanov's scheme develops quite large values.

5.5 Results for Test-case 5

	Region L	Region $-$	Region $+$	Region R
α_1	1.0	1.0	0.0	0.0
ρ_1	1.6	2.0	—	—
u_1	1.79057	1.0	—	—
p_1	5.0	10.0	—	—
ρ_2	—	—	2.0	2.67183
u_2	—	—	1.0	1.78888
p_2	—	—	10.0	15.0

Table 6: Test-case 5: Left, right and intermediate states of the exact solution.

The last test-case considers the coupling between two pure phases. A left region, where only phase 1 exists ($\alpha_{1,L} = 1$), is separated by a u_2 -contact discontinuity from a right region, where only phase 2 is present ($\alpha_{1,R} = 0$). In the existence region for each phase, the solution is composed of a shock.

In the numerical implementation, we set $\alpha_{1,L} = 1 - 10^{-9}$ and $\alpha_{1,R} = 10^{-9}$. In addition, in the LHS region, where phase 2 is absent, we choose to set $\rho_{2,L}$, $u_{2,L}$ and $p_{2,L}$ to the values on the right of the u_2 -contact discontinuity *i.e.* to the values ρ_2^+ , u_2^+ and p_2^+ . The symmetric choice is made for phase 1 in the RHS region: we set $\rho_{1,R} = \rho_1^-$, $u_{1,R} = u_1^-$ and $p_{1,R} = p_1^-$. Another choice could have been made for the initialization of the absent phase by imposing an instantaneous local thermodynamical equilibrium between the phases at time $t = 0$. This would be coherent with the relaxation zero-th order source terms that are usually added to the model when simulating practical industrial configurations.

One can see that, in the LHS region, the quantities of the only present phase 1 are correctly approximated while the quantities of the vanishing phase 2 remain stable despite the division by small values of α_2 . The same observation can be made for the RHS region. On the contrary, Rusanov's scheme fails to approximate such vanishing phase solution.

6 Conclusion

The work performed in [16] and in the present paper provides an accurate and robust finite volume scheme for approximating the entropy dissipating weak solutions of the Baer-Nunziato two-phase flow model. The scheme relies on an exact Riemann solver for a relaxation approximation *à la Suliciu* of the Baer-Nunziato model. Up to our knowledge, this is the only existing scheme for which the approximated phase fractions, phase densities and phase pressures are proven to remain positive without any smallness assumption on the data or on the phase fraction gradient. In addition, it

is the only scheme for which discrete counterparts of the entropy inequalities satisfied by the exact solutions of the model are proven for all thermodynamically admissible equations of state, under a fully computable CFL condition.

The scheme is well-adapted for subsonic flows (in terms of the relative velocity between the phases) and flows for which the phases are close to the thermodynamical and mechanical equilibrium, a state which is characterized by the equality of pressures, velocities and temperatures of both phases. This numerical method is therefore a natural candidate for simulating the convective part of the complete two-phase flow model, where zero-th order source terms are added to account for the relaxation phenomena that tend to bring the two phases towards thermodynamical and mechanical equilibria.

This scheme was specially designed for the simulation of vanishing phase solutions, where in some areas of the flow, the fluid is quasi monophasic *i.e.* one of the phases has nearly disappeared. In particular, the scheme has been proven to robustly handle sharp interfaces between two quasi monophasic regions as assessed by the results of Test-case 5 (see Section 5.5). Simulating vanishing phase solutions is a crucial issue for a detailed investigation of incidental configurations in the nuclear industry such as the Departure from Nucleate Boiling (DNB) [42], the Loss of Coolant Accident (LOCA) [43] or the Reactivity Initiated Accident (RIA) [31]. Some numerical methods had already been proposed for the approximation of vanishing phase solutions ([38, 41]). The work performed in [16] and in the present paper provides a detailed theoretical and numerical answer to the robustness issues rising up when attempting to simulate vanishing phase solutions.

Despite a relatively complex theory aiming at constructing the underlying approximate Riemann solver, and at analyzing the main properties of the numerical method (positivity, discrete entropy inequalities), the proposed scheme is a rather simple scheme as regards its practical implementation as explained in the appendices 7. The scheme applies for all equations of state for which the pressure is a given function of the density and of the specific internal energy. In particular, this allows the use of incomplete or tabulated equations of state.

The scheme compares very favorably with Lax-Friedrichs type schemes that are commonly used in the nuclear industry for their known robustness and simplicity. As a matter of fact, the relaxation finite volume scheme was proved to be much more accurate than Rusanov's scheme for the same level of refinement. In addition, for a prescribed level of accuracy (in terms of the L^1 -error for instance), the computational cost of the relaxation scheme is much lower than that of Rusanov's scheme. Indeed, for some test-cases, reaching the same level of accuracy on some variables may require more than a hundred times more CPU-time to Rusanov's scheme than to the relaxation scheme! In a recent benchmark on numerical methods for two-phase flows [2], the relaxation scheme was proven to compare very well with various other schemes in terms of CPU-time performances as well as robustness [17].

Thanks to the invariance of the Baer-Nunziato model under Galilean transformations, the finite volume formulation of the relaxation scheme allows a straightforward extension to 2D and 3D unstructured meshes. As a matter of fact, the scheme has already been implemented in a proprietary module for 3D two-phase flows developed by the French national electricity company EDF within the framework of the industrial CFD code *Code_Saturne* [1]. The scheme has been successfully applied within nuclear safety studies, for numerical simulations of the primary circuit of pressurized water reactors. A forthcoming paper is in preparation, where the relaxation scheme is used for the simulation of 3D industrial cases.

7 Appendices

7.1 Construction of the solution to the Riemann problem (24)-(30).

Given $(\mathbb{W}_L, \mathbb{W}_R, a_1, a_2)$ (satisfying $\mathcal{T}_{k,L} = \tau_{k,L}$ and $\mathcal{T}_{k,R} = \tau_{k,R}$ for $k \in \{1, 2\}$) such that the conditions of Theorem 3.5 are met, we display the expression of the piecewise constant solution of the Riemann problem (24)-(30). For the sake of simplicity, the solution will be expressed in non conservative variables $\mathcal{W} = (\alpha_1, \tau_1, \tau_2, u_1, u_2, \pi_1, \pi_2, \mathcal{E}_1, \mathcal{E}_2)$.

In practice, when implementing the numerical scheme, the relaxation Riemann solution of (24)-

(30) is used to compute the numerical fluxes at each interface between two states $(\mathcal{U}_L, \mathcal{U}_R)$ and the relaxation states $(\mathbb{W}_L, \mathbb{W}_R)$ are actually computed from these two states $(\mathcal{U}_L, \mathcal{U}_R)$. For this reason, the solution will be denoted

$$\xi \longmapsto \widetilde{\mathcal{W}}(\xi; \mathcal{U}_L, \mathcal{U}_R; a_1, a_2).$$

We recall the following notations built on the initial states $(\mathbb{W}_L, \mathbb{W}_R)$ (and therefore depending on $(\mathcal{U}_L, \mathcal{U}_R)$) and on the relaxation parameters (a_1, a_2) , which are useful for the computation of the solution.

For k in $\{1, 2\}$:

$$\begin{aligned} u_k^\sharp(\mathcal{U}_L, \mathcal{U}_R; a_k) &:= \frac{1}{2}(u_{k,L} + u_{k,R}) - \frac{1}{2a_k}(p_{k,R} - p_{k,L}), \\ \pi_k^\sharp(\mathcal{U}_L, \mathcal{U}_R; a_k) &:= \frac{1}{2}(p_{k,R} + p_{k,L}) - \frac{a_k}{2}(u_{k,R} - u_{k,L}), \\ \tau_{k,L}^\sharp(\mathcal{U}_L, \mathcal{U}_R; a_k) &:= \tau_{k,L} + \frac{1}{a_k}(u_k^\sharp(\mathcal{U}_L, \mathcal{U}_R; a_k) - u_{k,L}), \\ \tau_{k,R}^\sharp(\mathcal{U}_L, \mathcal{U}_R; a_k) &:= \tau_{k,R} - \frac{1}{a_k}(u_k^\sharp(\mathcal{U}_L, \mathcal{U}_R; a_k) - u_{k,R}). \end{aligned} \tag{77}$$

We also recall the notations:

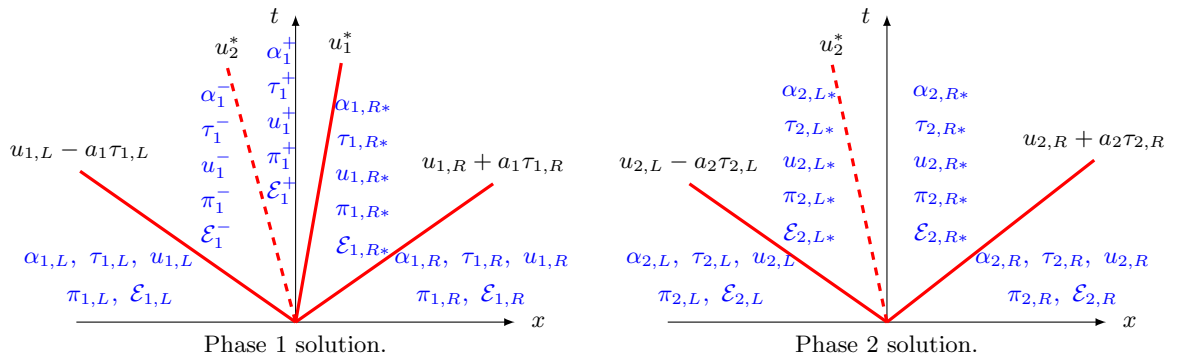
$$\begin{aligned} \Lambda^\alpha(\mathcal{U}_L, \mathcal{U}_R) &:= \frac{\alpha_{2,R} - \alpha_{2,L}}{\alpha_{2,R} + \alpha_{2,L}}, \\ U^\sharp(\mathcal{U}_L, \mathcal{U}_R; a_1, a_2) &:= \frac{u_1^\sharp(\mathcal{U}_L, \mathcal{U}_R; a_1) - u_2^\sharp(\mathcal{U}_L, \mathcal{U}_R; a_2) - \frac{1}{a_2}\Lambda^\alpha(\mathcal{U}_L, \mathcal{U}_R)(\pi_1^\sharp(\mathcal{U}_L, \mathcal{U}_R; a_1) - \pi_2^\sharp(\mathcal{U}_L, \mathcal{U}_R; a_2))}{1 + \frac{a_1}{a_2}|\Lambda^\alpha(\mathcal{U}_L, \mathcal{U}_R)|}. \end{aligned} \tag{78}$$

Later in this section, we will omit the dependency of these quantities on $(\mathcal{U}_L, \mathcal{U}_R; a_1, a_2)$. Following Theorem 3.5, if a_1 and a_2 are such that $\tau_{1,L}^\sharp, \tau_{1,R}^\sharp, \tau_{2,L}^\sharp, \tau_{2,R}^\sharp$ are positive, and if condition **(A)** which reads $-a_1\tau_{1,R}^\sharp < U^\sharp < a_1\tau_{1,L}^\sharp$ holds true, then there exists a self-similar solution to the Riemann problem (24)-(30). Following [16], we distinguish three different cases corresponding to different orderings of the kinematic waves, $u_1^* < u_2^*$, $u_1^* = u_2^*$ or $u_1^* > u_2^*$. With each one of these wave configurations is associated a different expression of assumption **(A)** depending on the sign of U^\sharp .

Solution with the wave ordering $u_2^* < u_1^*$:

The solution $\xi \mapsto \widetilde{\mathcal{W}}(\xi; \mathcal{U}_L, \mathcal{U}_R; a_1, a_2)$ has the wave ordering $u_2^* < u_1^*$ if the following assumption holds:

$$\text{(A1)} \quad 0 < U^\sharp < a_1\tau_{1,L}^\sharp.$$



The intermediate states, which are represented in the above figure, and the velocities $u_1^*(\mathcal{U}_L, \mathcal{U}_R; a_1, a_2)$ and $u_2^*(\mathcal{U}_L, \mathcal{U}_R; a_1, a_2)$ (simply denoted u_1^* and u_2^* hereafter) are computed through the following steps performed in the very same order.

1. Define $\nu := \frac{\alpha_{1,L}}{\alpha_{1,R}}$, $\mathcal{M}_L^\sharp := \frac{u_1^\sharp - u_2^\sharp}{a_1 \tau_{1,L}^\sharp}$ and $\mathcal{P}_L^\sharp := \frac{\pi_1^\sharp - \pi_2^\sharp}{a_1^2 \tau_{1,L}^\sharp}$.
2. Define successively the functions

$$\begin{aligned} \mathcal{M}_0(\omega) &:= \frac{1}{2} \left(\frac{1+\omega^2}{1-\omega^2} \left(1 + \frac{1}{\nu}\right) - \sqrt{\left(\frac{1+\omega^2}{1-\omega^2}\right)^2 \left(1 + \frac{1}{\nu}\right)^2 - \frac{4}{\nu}} \right), \\ \mathcal{M}_\mu(m) &:= \frac{1}{\nu} \frac{m + (1-\mu) \frac{\tau_{1,R}^\sharp}{\tau_{1,L}^\sharp}}{1 - (1-\mu) \frac{\tau_{1,R}^\sharp}{\tau_{1,L}^\sharp}}, \quad \text{with } \mu \in (0, 1). \text{ For instance } \mu = 0.1, \\ \mathcal{M}(m) &:= \min \left(\mathcal{M}_0 \left(\frac{1-m}{1+m} \right), \mathcal{M}_\mu(m) \right), \\ \Psi(m) &:= m + \frac{a_1}{a_2} \frac{\alpha_{1,R}}{\alpha_{2,L} + \alpha_{2,R}} ((1+\nu)m - 2\nu \mathcal{M}(m)). \end{aligned}$$

3. Use an iterative method (e.g. Newton's method or a dichotomy algorithm) to compute $\mathcal{M}_L^* \in (0, 1)$ such that

$$\Psi(\mathcal{M}_L^*) = \mathcal{M}_L^\sharp - \frac{a_1}{a_2} \Lambda^\alpha \mathcal{P}_L^\sharp. \quad (79)$$

According to [16], \mathcal{M}_L^* always exists under **(A1)** and is unique if μ is close enough to one. In practice, the iterative method is initialized at $m^0 = \max(0, \min(\mathcal{M}_L^\sharp, 1))$.

4. The velocity u_2^* is obtained by $u_2^* = u_1^\sharp - a_1 \tau_{1,L}^\sharp \mathcal{M}_L^*$.
5. The velocity u_1^* is obtained by $u_1^* = u_2^* + \nu a_1 \tau_{1,L}^\sharp \mathcal{M}(\mathcal{M}_L^*) \frac{1 - \mathcal{M}_L^*}{1 - \mathcal{M}(\mathcal{M}_L^*)}$.
6. The intermediate states for phase 1 are given by

- Phase fractions: $\alpha_1^- = \alpha_{1,L}$, $\alpha_1^+ = \alpha_{1,R^*} = \alpha_{1,R}$.
- Specific volumes:

$$\tau_1^- = \tau_{1,L}^\sharp \frac{1 - \mathcal{M}_L^*}{1 - \mathcal{M}(\mathcal{M}_L^*)}, \quad \tau_1^+ = \tau_{1,L}^\sharp \frac{1 + \mathcal{M}_L^*}{1 + \nu \mathcal{M}(\mathcal{M}_L^*)}, \quad \tau_{1,R^*} = \tau_{1,R}^\sharp + \tau_{1,L}^\sharp \frac{\mathcal{M}_L^* - \nu \mathcal{M}(\mathcal{M}_L^*)}{1 + \nu \mathcal{M}(\mathcal{M}_L^*)}.$$

- Velocities:

$$u_1^- = u_2^* + a_1 \tau_{1,L}^\sharp \mathcal{M}(\mathcal{M}_L^*) \frac{1 - \mathcal{M}_L^*}{1 - \mathcal{M}(\mathcal{M}_L^*)}, \quad u_1^+ = u_{1,R^*} = u_1^*.$$

- Relaxation pressures $\pi_1(\tau_1, \mathcal{T}_1, s_1)$:

$$\pi_1^- = p_{1,L} + a_1^2 (\tau_{1,L} - \tau_1^-), \quad \pi_1^+ = p_{1,L} + a_1^2 (\tau_{1,L} - \tau_1^+), \quad \pi_{1,R^*} = p_{1,R} + a_1^2 (\tau_{1,R} - \tau_{1,R^*}).$$

- Relaxation total energies $\mathcal{E}_1(u_1, \tau_1, \mathcal{T}_1, s_1)$:

$$\begin{aligned} \mathcal{E}_1^- &= (u_1^-)^2/2 + e_{1,L} + ((\pi_1^-)^2 - p_{1,L}^2)/(2a_1^2), \\ \mathcal{E}_1^+ &= (u_1^+)^2/2 + e_{1,L} + ((\pi_1^+)^2 - p_{1,L}^2)/(2a_1^2), \\ \mathcal{E}_{1,R^*} &= (u_{1,R^*})^2/2 + e_{1,R} + (\pi_{1,R^*}^2 - p_{1,R}^2)/(2a_1^2). \end{aligned}$$

7. The intermediate states for phase 2 are then given by

- Specific volumes: $\tau_{2,L*} = \tau_{2,L} + \frac{1}{a_2}(u_2^* - u_{2,L})$, $\tau_{2,R*} = \tau_{2,R} - \frac{1}{a_2}(u_2^* - u_{2,R})$.
- Velocities: $u_{2,L*} = u_{2,R*} = u_2^*$.
- Relaxation pressures $\pi_2(\tau_2, \mathcal{T}_2, s_2)$:

$$\pi_{2,L*} = p_{2,R} + a_2^2(\tau_{2,L} - \tau_{2,L*}), \quad \pi_{2,R*} = p_{2,R} + a_2^2(\tau_{2,R} - \tau_{2,R*}).$$

- Relaxation total energies $\mathcal{E}_2(u_2, \tau_2, \mathcal{T}_2, s_2)$:

$$\begin{aligned} \mathcal{E}_{2,L*} &= (u_2^*)^2/2 + e_{2,L} + (\pi_{2,L*}^2 - p_{2,L}^2)/(2a_2^2), \\ \mathcal{E}_{2,R*} &= (u_2^*)^2/2 + e_{2,R} + (\pi_{2,R*}^2 - p_{2,R}^2)/(2a_2^2). \end{aligned}$$

Solution with the wave ordering $u_2^* > u_1^*$:

The solution $\xi \mapsto \widetilde{\mathcal{W}}(\xi; \mathcal{U}_L, \mathcal{U}_R; a_1, a_2)$ has the wave ordering $u_2^* > u_1^*$ if the following assumption holds:

$$(A2) \quad -a_1\tau_{1,R}^\sharp < U^\sharp < 0.$$

For the determination of the wave velocities and the intermediate states, the simplest thing to do is to exploit the Galilean invariance of the equations. In this case indeed, the solution is obtained by the transformation

$$\widetilde{\mathcal{W}}(\xi; \mathcal{U}_L, \mathcal{U}_R; a_1, a_2) := \mathcal{V}\widetilde{\mathcal{W}}(-\xi; \mathcal{V}\mathcal{U}_R, \mathcal{V}\mathcal{U}_L; a_1, a_2), \quad (80)$$

where the operator \mathcal{V} changes the velocities into their opposite values:

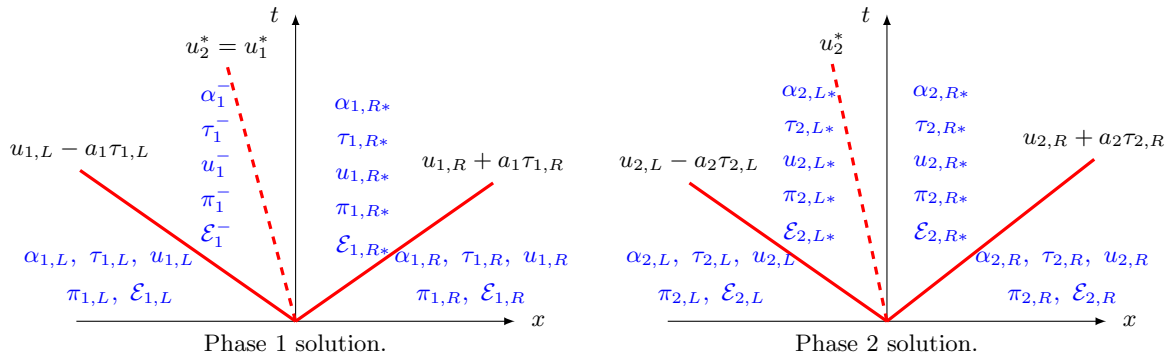
$$\mathcal{V} : (x_1, x_2, x_3, x_4, x_5, x_6, x_7, x_8, x_9) \mapsto (x_1, x_2, x_3, -x_4, -x_5, x_6, x_7, x_8, x_9). \quad (81)$$

Of course, the function $\xi \mapsto \widetilde{\mathcal{W}}(\xi; \mathcal{V}\mathcal{U}_R, \mathcal{V}\mathcal{U}_L; a_1, a_2)$ is computed through the first case, since for these new initial data $(\mathcal{V}\mathcal{U}_R, \mathcal{V}\mathcal{U}_L)$, it is condition (A1) that holds.

Solution with the wave ordering $u_2^* = u_1^*$:

The solution $\xi \mapsto \widetilde{\mathcal{W}}(\xi; \mathcal{U}_L, \mathcal{U}_R; a_1, a_2)$ has the wave ordering $u_2^* = u_1^*$ if the following assumption holds:

$$(A3) \quad U^\sharp = 0.$$



The kinematic velocities are given by $u_2^* = u_1^* = u_1^\sharp$. The intermediate states for phase 2 are obtained by the same formulae as in the case $u_2^* < u_1^*$, while the intermediate states for phase 1 read

$$\begin{aligned} \alpha_1^- &= \alpha_{1,L}, & \alpha_{1,R^*} &= \alpha_{1,R}, \\ \tau_1^- &= \tau_{1,L}^\sharp, & \tau_{1,R^*} &= \tau_{1,R}^\sharp, \\ u_1^- &= u_1^\sharp, & u_{1,R^*} &= u_1^\sharp, \\ \pi_1^- &= p_{1,L} + a_1^2(\tau_{1,L} - \tau_{1,L}^\sharp), & \pi_{1,R^*} &= p_{1,R} + a_1^2(\tau_{1,R} - \tau_{1,R^*}^\sharp), \\ \mathcal{E}_1^- &= (u_1^-)^2/2 + e_{1,L} + ((\pi_1^-)^2 - p_{1,L}^2)/(2a_1^2), & \mathcal{E}_{1,R^*} &= (u_{1,R^*})^2/2 + e_{1,R} + (\pi_{1,R^*}^2 - p_{1,R}^2)/(2a_1^2). \end{aligned}$$

The non-conservative product $\mathbf{d}(\mathbb{W})\partial_x \mathbb{W}$:

When $\alpha_{1,L} \neq \alpha_{1,R}$, the non-conservative product $\mathbf{d}(\mathbb{W})\partial_x \mathbb{W}$ identifies with a Dirac measure propagating at the constant velocity u_2^* . This Dirac measure is given by

$$\mathbf{D}^*(\mathbb{W}_L, \mathbb{W}_R)\delta_{x-u_2^*t},$$

where $\mathbf{D}^*(\mathbb{W}_L, \mathbb{W}_R) := (\alpha_{1,R} - \alpha_{1,L})(u_2^*, 0, 0, -\pi_1^*, +\pi_1^*, 0, 0, 0, 0)^T$. The pressure π_1^* is defined for $\alpha_{1,R} \neq \alpha_{1,L}$ by

$$\pi_1^* := \pi_2^\sharp - a_2 \frac{\alpha_{2,R} + \alpha_{2,L}}{\alpha_{1,R} - \alpha_{1,L}}(u_2^* - u_2^\sharp).$$

7.2 Practical implementation of the relaxation finite volume scheme

In this appendix, we describe in detail the practical implementation of the scheme. We recall the space and time discretization: we assume a positive space step Δx and the time step Δt is dynamically updated through the CFL condition. The space is partitioned into cells $\mathbb{R} = \bigcup_{j \in \mathbb{Z}} [x_{j-\frac{1}{2}}, x_{j+\frac{1}{2}}[$ with $x_{j+\frac{1}{2}} = (j + \frac{1}{2})\Delta x$ for all j in \mathbb{Z} . The centers of the cells are denoted $x_j = j\Delta x$ for all j in \mathbb{Z} . We also introduce the discrete intermediate times $t^n = n\Delta t$, $n \in \mathbb{N}$.

The solution of the Cauchy problem:

$$\begin{cases} \partial_t \mathcal{U} + \partial_x \mathcal{F}(\mathcal{U}) + \mathcal{C}(\mathcal{U})\partial_x \mathcal{U} = 0, & x \in \mathbb{R}, t > 0, \\ \mathcal{U}(x, 0) = \mathcal{U}_0(x), & x \in \mathbb{R}, \end{cases}$$

is approximated at time t^n by \mathcal{U}_j^n on the cell $[x_{j-\frac{1}{2}}, x_{j+\frac{1}{2}}[$. The values of the approximate solution are inductively computed as follows:

Initialization:

$$\mathcal{U}_j^0 = \frac{1}{\Delta x} \int_{x_{j-\frac{1}{2}}}^{x_{j+\frac{1}{2}}} \mathcal{U}_0(x) dx.$$

Time evolution:

$$\mathcal{U}_j^{n+1} = \mathcal{U}_j^n - \frac{\Delta t}{\Delta x} (\mathcal{F}^-(\mathcal{U}_j^n, \mathcal{U}_{j+1}^n) - \mathcal{F}^+(\mathcal{U}_{j-1}^n, \mathcal{U}_j^n)). \quad (82)$$

At each cell interface $x_{j+\frac{1}{2}}$, the numerical fluxes $\mathcal{F}^\pm(\mathcal{U}_j^n, \mathcal{U}_{j+1}^n)$ are computed thanks to the relaxation approximate Riemann solver. They depend on the states $(\mathcal{U}_j^n, \mathcal{U}_{j+1}^n)$ but also on the local values of the relaxation parameters $a_{k,j+\frac{1}{2}}^n$, $k = 1, 2$. Denoting $\mathcal{U}_L = \mathcal{U}_j^n$ and $\mathcal{U}_R = \mathcal{U}_{j+1}^n$ and a_k , $k = 1, 2$ for simplicity, the fluxes $\mathcal{F}^\pm(\mathcal{U}_L, \mathcal{U}_R)$ are computed through the following steps.

1. *Local choice of the pair (a_1, a_2) .* The pair of parameters (a_1, a_2) , must be chosen large enough so as to satisfy several requirements:

- In order to ensure the stability of the relaxation approximation, a_k must satisfy Whitham's condition (62). For simplicity however, we do not impose Whitham's condition everywhere in the solution of the Riemann problem (24)-(30) (which is possible however), but only for the left and right initial data at each interface:

$$\text{for } k \text{ in } \{1, 2\}, \quad a_k > \max(\rho_{k,L} c_k(\rho_{k,L}, e_{k,L}), \rho_{k,R} c_k(\rho_{k,L}, e_{k,L})), \quad (83)$$

where $c_k(\rho_k, e_k)$ is the speed of sound in phase k . In practice, no instabilities were observed during the numerical simulations due to this simpler Whitham-like condition.

- In order to compute the solution of the relaxation Riemann problem, the specific volumes $\tau_{k,L}^\#(\mathcal{U}_L, \mathcal{U}_R; a_k)$ and $\tau_{k,R}^\#(\mathcal{U}_L, \mathcal{U}_R; a_k)$ defined in (77) must be positive. The expressions of $\tau_{k,L}^\#(\mathcal{U}_L, \mathcal{U}_R; a_k)$ and $\tau_{k,R}^\#(\mathcal{U}_L, \mathcal{U}_R; a_k)$ are two second order polynomials in a_k^{-1} whose constant terms are respectively $\tau_{k,L}$ and $\tau_{k,R}$. Hence, by taking a_k large enough, one can guarantee that $\tau_{k,L}^\#(\mathcal{U}_L, \mathcal{U}_R; a_k) > 0$ and $\tau_{k,R}^\#(\mathcal{U}_L, \mathcal{U}_R; a_k) > 0$, since the initial specific volumes $\tau_{k,L}$ and $\tau_{k,R}$ are positive.
- Finally, in order for the relaxation Riemann problem (24)-(30) to have a positive solution, (a_1, a_2) must be chosen so as to meet the condition **(A)** of Theorem 3.5 as well as the positivity condition of the phase 2 densities **(B)** (see the comments after Theorem 3.5).

Thereafter, we propose an iterative algorithm for the computation of the parameters (a_1, a_2) at each interface. The notation $\text{not}(\mathbf{P})$ is the negation of the logical statement \mathbf{P} .

- Choose η a (small) parameter in the interval $(0, 1)$.
- For k in $\{1, 2\}$ initialize a_k :
$$a_k := (1 + \eta) \max(\rho_{k,L} c_k(\rho_{k,L}, e_{k,L}), \rho_{k,R} c_k(\rho_{k,R}, e_{k,R})).$$
- For k in $\{1, 2\}$:
 - do $\{a_k := (1 + \eta)a_k\}$ while $(\tau_{k,L}^\#(\mathcal{U}_L, \mathcal{U}_R; a_k) \leq 0 \text{ or } \tau_{k,R}^\#(\mathcal{U}_L, \mathcal{U}_R; a_k) \leq 0)$.
- do $\{a_2 := (1 + \eta)a_2,$
 - do $\{a_1 := (1 + \eta)a_1\}$ while $(\text{not}(\mathbf{A}))$,
 - compute the value of u_2^* in the solution $\widetilde{\mathcal{W}}(\mathcal{U}_L, \mathcal{U}_R; a_1, a_2)$,
 - $\}$ while $(\text{not}(\mathbf{B}))$.

In this algorithm, the computation of u_2^* requires the computation of the solution of the fixed-point problem (79), using some numerical method such as Newton's method or a dichotomy algorithm. It is possible to prove that this algorithm always converges in the sense that there is no infinite looping due to the while-conditions. Indeed, it is easy to observe that assumptions **(A)** and **(B)** are always satisfied if the parameters (a_1, a_2) are taken large enough. Moreover, this algorithm provides reasonable values of a_1 and a_2 , since in all the numerical simulations, the time step obtained through the CFL condition (55) remains reasonably large and does not go to zero. In fact, the obtained values of a_1 and a_2 are quite satisfying since the relaxation scheme compares very favorably with Rusanov's scheme, in terms of CPU-time performances (see Section 5).

2. *Calculation of the numerical fluxes.* Once the relaxation parameters are known, one may give the expressions of the numerical fluxes $\mathcal{F}^\pm(\mathcal{U}_L, \mathcal{U}_R)$. Observe that, as a by-product of the above algorithm for the computation of (a_1, a_2) , the propagation velocity u_2^* is already known, and one does not need to redo the fixed-point procedure. Given the solution $\xi \mapsto \widetilde{\mathcal{W}}(\xi; \mathcal{U}_L, \mathcal{U}_R; a_1, a_2)$ of the relaxation Riemann problem (24)-(30) (see appendix 7.1 for the expression of the intermediate states), which we denote $\widetilde{\mathcal{W}}(\xi)$ for the sake of simplicity, the numerical fluxes are computed as

follows:

$$\mathcal{F}^\pm(\mathcal{U}_L, \mathcal{U}_R) = \begin{bmatrix} 0 \\ \alpha_1 \rho_1 u_1(\widetilde{\mathcal{W}}(0^\pm)) \\ \alpha_2 \rho_2 u_2(\widetilde{\mathcal{W}}(0^\pm)) \\ \alpha_1 \rho_1 u_1^2 + \alpha_1 \pi_1(\widetilde{\mathcal{W}}(0^\pm)) \\ \alpha_2 \rho_2 u_2^2 + \alpha_2 \pi_2(\widetilde{\mathcal{W}}(0^\pm)) \\ \alpha_1 \rho_1 \mathcal{E}_1 u_1 + \alpha_1 \pi_1 u_1(\widetilde{\mathcal{W}}(0^+)) \\ \alpha_2 \rho_2 \mathcal{E}_2 u_2 + \alpha_2 \pi_2 u_2(\widetilde{\mathcal{W}}(0^+)) \end{bmatrix} + \begin{bmatrix} (u_2^*)^\pm \\ 0 \\ 0 \\ -\frac{(u_2^*)^\pm}{u_2^*} \pi_1^* \\ \frac{(u_2^*)^\pm}{u_2^*} \pi_1^* \\ -(u_2^*)^\pm \pi_1^* \\ (u_2^*)^\pm \pi_1^* \end{bmatrix} (\alpha_{1,R} - \alpha_{1,L}),$$

where u_2^* is already known as a result of the first step (choice of the pair (a_1, a_2)) and the expression of π_1^* is given at the end of appendix 7.1. In the above expression of the numerical fluxes, we have denoted $(u_2^*)^+ = \max(u_2^*, 0)$, $(u_2^*)^- = \min(u_2^*, 0)$ and the functions $x \mapsto \frac{(x)^\pm}{x}$ are extended by 0 at $x = 0$.

Finally, the time step is computed so as to satisfy the CFL condition:

$$\frac{\Delta t}{\Delta x} \max_{k \in \{1,2\}, j \in \mathbb{Z}} \max \{ |(u_k - a_k \tau_k)_j^n|, |(u_k + a_k \tau_k)_{j+1}^n| \} < \frac{1}{2},$$

and the scheme (82) can be now applied to update the values of the unknown \mathcal{U}_j^{n+1} for $j \in \mathbb{Z}$.

Acknowledgements. The authors would like to thank Nicolas Seguin who is a co-author of [16] upon which the present paper is based. The authors would like to thank him for his thorough reading of this paper which has constantly led to improving the text. This work has been partially funded by ANRT and EDF through an EDF-CIFRE contract 529/2009.

References

- [1] Code_Sturme : a finite volume code for the computation of turbulent incompressible flows - industrial applications. *International Journal on Finite Volumes*, 2004.
- [2] Atelier de vérification de schémas pour la simulation des modèles diphasiques, Chatou – 2015. <https://www.i2m.univ-amu.fr/Atelier-de-verification-de-schemas-pour-la?lang=fr>.
- [3] R. Abgrall and S. Dallet. Large time-step numerical scheme for the seven-equation model of compressible two-phase flows. *Finite Volumes for Complex Applications VII, Parabolic and Hyperbolic Problems*, pages 749–757, 2014.
- [4] R. Abgrall and R. Saurel. Discrete equations for physical and numerical compressible multiphase mixtures. *Journal of Computational Physics*, 186(2):361–396, 2003.
- [5] A. Ambroso, C. Chalons, F. Coquel, and T. Galié. Relaxation and numerical approximation of a two-fluid two-pressure diphasic model. *M2AN Math. Model. Numer. Anal.*, 43(6):1063–1097, 2009.
- [6] A. Ambroso, C. Chalons, and P.-A. Raviart. A Godunov-type method for the seven-equation model of compressible two-phase flow. *Computers and Fluids*, 54(0):67 – 91, 2012.
- [7] N. Andrianov and G. Warnecke. The Riemann problem for the Baer-Nunziato two-phase flow model. *J. Comput. Phys.*, 195(2):434–464, 2004.
- [8] T. Asmaa. PhD thesis, Université Pierre et Marie Curie, to appear.

- [9] M.R. Baer and J.W. Nunziato. A two-phase mixture theory for the deflagration-to-detonation transition (DDT) in reactive granular materials. *International Journal of Multiphase Flow*, 12(6):861 – 889, 1986.
- [10] F. Bouchut. *Nonlinear stability of finite volume methods for hyperbolic conservation laws and well-balanced schemes for sources*. Frontiers in Mathematics. Birkhäuser Verlag, Basel, 2004.
- [11] C. Chalons, F. Coquel, S. Kokh, and N. Spillane. Large time-step numerical scheme for the seven-equation model of compressible two-phase flows. *Springer Proceedings in Mathematics, FVCA 6, 2011*, 4:225–233, 2011.
- [12] F. Coquel, T. Gallouët, J-M. Hérard, and N. Seguin. Closure laws for a two-fluid two pressure model. *C. R. Acad. Sci.*, I-334(5):927–932, 2002.
- [13] F. Coquel, E. Godlewski, B. Perthame, A. In, and P. Rascle. Some new Godunov and relaxation methods for two-phase flow problems. In *Godunov methods (Oxford, 1999)*, pages 179–188. Kluwer/Plenum, New York, 2001.
- [14] F. Coquel, E. Godlewski, and N. Seguin. Relaxation of fluid systems. *Math. Models Methods Appl. Sci.*, 22(8), 2012.
- [15] F. Coquel, J-M. Hérard, and K. Saleh. A splitting method for the isentropic Baer-Nunziato two-phase flow model. *ESAIM: Proc.*, 38:241–256, 2012.
- [16] F. Coquel, J-M. Hérard, K. Saleh, and N. Seguin. A robust entropy-satisfying finite volume scheme for the isentropic Baer-Nunziato model. *ESAIM: Mathematical Modelling and Numerical Analysis*, eFirst, 7 2013.
- [17] S. Dallet. A comparative study of numerical schemes for the Baer-Nunziato model. *Int. Journ. on Finite Volumes*, to appear.
- [18] F. Daude and P. Galon. On the Computation of the Baer-Nunziato Model Using ALE Formulation with HLL- and HLLC-type Solvers Towards Fluid-structure Interactions. *J. Comput. Phys.*, 304(C):189–230, January 2016.
- [19] M. Dumbser, A. Hidalgo, M. Castro, C. Parés, and E.F. Toro. FORCE schemes on unstructured meshes II: Non-conservative hyperbolic systems. *Computer Methods in Applied Mechanics and Engineering*, 199(9–12):625–647, 2010.
- [20] P. Embid and M. Baer. Mathematical analysis of a two-phase continuum mixture theory. *Contin. Mech. Thermodyn.*, 4(4):279–312, 1992.
- [21] T. Flåtten and H. Lund. Relaxation two-phase flow models and the subcharacteristic condition. *Mathematical Models and Methods in Applied Sciences*, 21(12):2379–2407, 2011.
- [22] E. Franquet and V. Perrier. Rungekutta discontinuous galerkin method for the approximation of Baer and Nunziato type multiphase models. *Journal of Computational Physics*, 231(11):4096 – 4141, 2012.
- [23] T. Gallouët, J-M. Hérard, and N. Seguin. Numerical modeling of two-phase flows using the two-fluid two-pressure approach. *Math. Models Methods Appl. Sci.*, 14(5):663–700, 2004.
- [24] S. Gavrilyuk and R. Saurel. Mathematical and numerical modeling of two-phase compressible flows with micro-inertia. *Journal of Computational Physics*, 175(1):326 – 360, 2002.
- [25] J. Glimm, D. Saltz, and D. H. Sharp. Renormalization group solution of two-phase flow equations for Rayleigh-taylor mixing. *Physics Letters A*, 222(3):171 – 176, 1996.
- [26] E. Godlewski and P.-A. Raviart. *Numerical approximation of hyperbolic systems of conservation laws*, volume 118 of *Applied Mathematical Sciences*. Springer-Verlag, New York, 1996.
- [27] E. Han, M. Hantke, and S. Müller. Modeling of multi-component flows with phase transition and application to collapsing bubbles. *Institut für Geometrie und Praktische Mathematik Preprint No. 409*, 2014.
- [28] A. Harten, P. D. Lax, and B. van Leer. On upstream differencing and Godunov-type schemes for hyperbolic conservation laws. *SIAM Rev.*, 25(1):35–61, 1983.

- [29] J.-M. Hérard. A three-phase flow model. *Mathematical and Computer Modelling*, 45(56):732 – 755, 2007.
- [30] J.-M. Hérard and O. Hurisse. A fractional step method to compute a class of compressible gas-liquid flows. *Computers & Fluids. An International Journal*, 55:57–69, 2012.
- [31] Institut de Radioprotection et de Sûreté Nucléaire (IRSN). Reactivity Initiated Accident (RIA). http://www.irsn.fr/FR/base_de_connaissances/Installations_nucleaires/Les-centrales-nucleaires/criteres_surete_ria_aprp/Pages/1-accident-reativite-RIA.aspx?dId=69fe2952-0491-4b2d-92f6-942f26aa8a84&dwId=985263bc-5429-4a6f-9037-df760ee8780d#.VrinKZNax6Wl.
- [32] S. Jin and Z. P. Xin. The relaxation schemes for systems of conservation laws in arbitrary space dimensions. *Comm. Pure Appl. Math.*, 48(3):235–276, 1995.
- [33] A. K. Kapila, S. F. Son, J. B. Bdzil, R. Menikoff, and D. S. Stewart. Two-phase modeling of DDT: Structure of the velocity-relaxation zone. *Physics of Fluids*, 9(12):3885–3897, 1997.
- [34] Y. Liu. *Contribution à la vérification et à la validation d’un modèle diphasique bifluide instationnaire*. PhD thesis, Université Aix-Marseille, 2013. <https://tel.archives-ouvertes.fr/tel-00864567/>.
- [35] S. Müller, M. Hantke, and P. Richter. Closure conditions for non-equilibrium multi-component models. *Continuum Mechanics and Thermodynamics*, pages 1–33, 2015.
- [36] K. Saleh. *Analyse et Simulation Numérique par Relaxation d’Écoulements Diphasiques Compressibles. Contribution au Traitement des Phases Évanescentes*. PhD thesis, Université Pierre et Marie Curie, Paris VI, 2012. <https://tel.archives-ouvertes.fr/tel-00761099/>.
- [37] R. Saurel and R. Abgrall. A multiphase godunov method for compressible multifluid and multiphase flows. *Journal of Computational Physics*, 150(2):425 – 467, 1999.
- [38] D.W. Schwendeman, C.W. Wahle, and A.K. Kapila. The Riemann problem and a high-resolution Godunov method for a model of compressible two-phase flow. *Journal of Computational Physics*, 212(2):490 – 526, 2006.
- [39] M.D. Thanh, D. Kröner, and C. Chalons. A robust numerical method for approximating solutions of a model of two-phase flows and its properties. *Applied Mathematics and Computation*, 219(1):320 – 344, 2012.
- [40] M.D. Thanh, D. Kröner, and N. T. Nam. Numerical approximation for a Baer–Nunziato model of two-phase flows. *Applied Numerical Mathematics*, 61(5):702 – 721, 2011.
- [41] S.A. Tokareva and E.F. Toro. HLLC-type Riemann solver for the Baer–Nunziato equations of compressible two-phase flow. *Journal of Computational Physics*, 229(10):3573 – 3604, 2010.
- [42] U.S. NRC: Glossary. Departure from Nucleate Boiling (DNB). <http://www.nrc.gov/reading-rm/basic-ref/glossary/departure-from-nucleate-boiling-dnb.html>.
- [43] U.S. NRC: Glossary. Loss of Coolant Accident (LOCA). <http://www.nrc.gov/reading-rm/basic-ref/glossary/loss-of-coolant-accident-loca.html>.

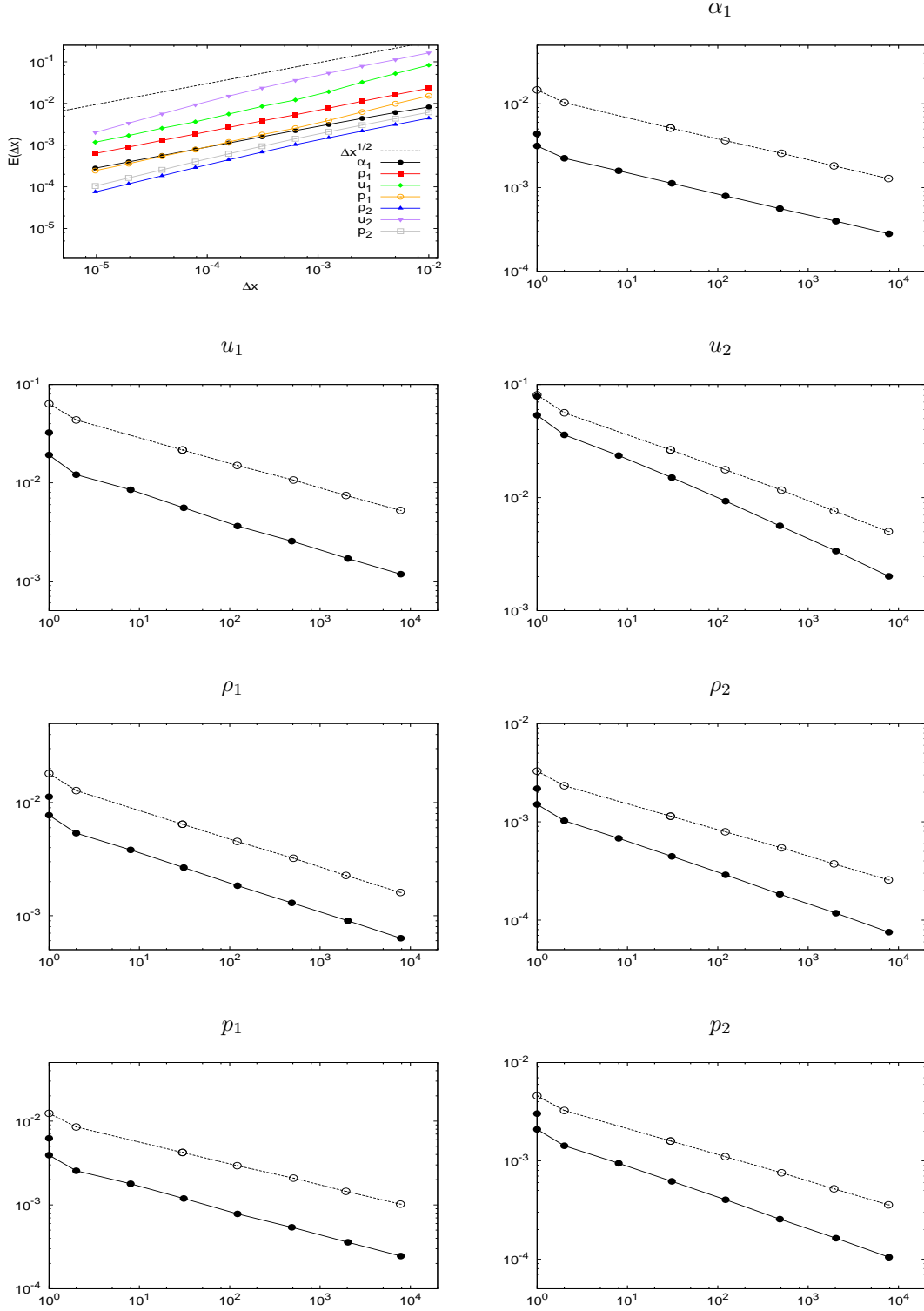


Figure 3: Test-case 1: L^1 -Error with respect to Δx and L^1 -Error with respect to computational cost (in seconds), straight line : relaxation scheme, dashed line : Rusanov's scheme.

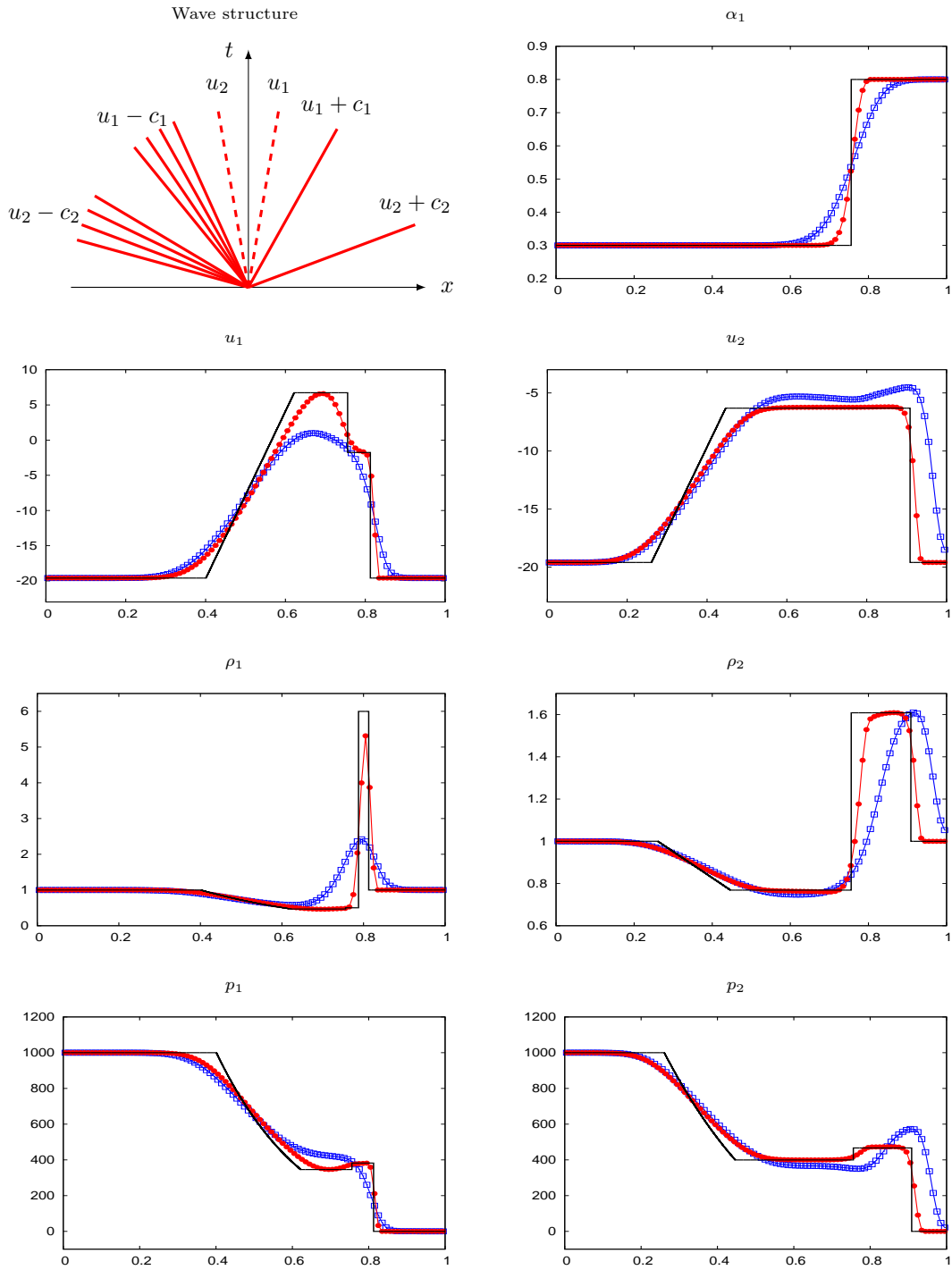


Figure 4: Test-case 2: Structure of the solution and space variations of the physical variables at the final time $T_{\max} = 0.007$. Mesh size: 100 cells. Straight line: exact solution, bullets: relaxation scheme, squares: Rusanov's scheme.

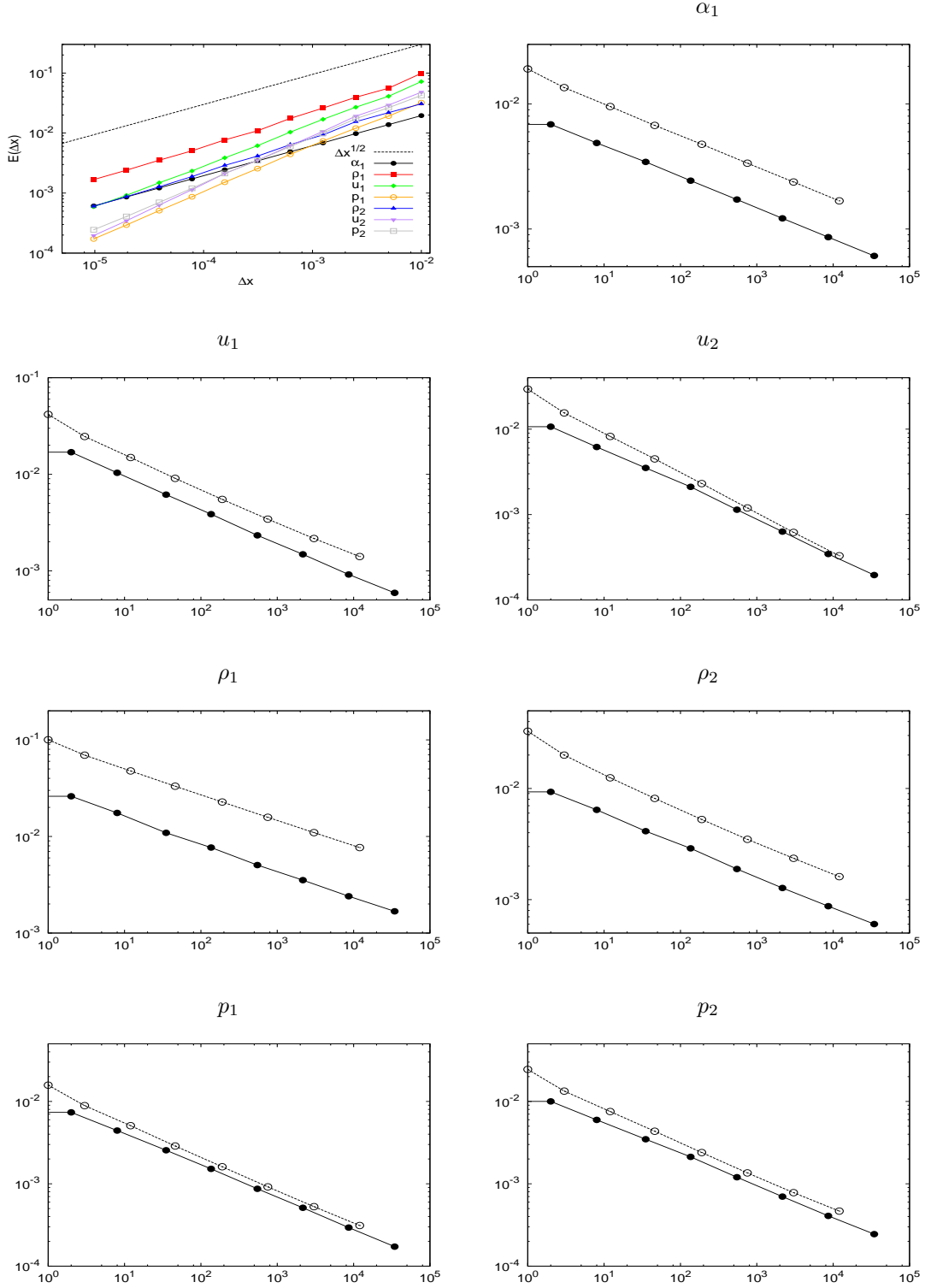


Figure 5: Test-case 2: L^1 -Error with respect to Δx and L^1 -Error with respect to computational cost (in seconds), straight line : relaxation scheme, dashed line : Rusanov's scheme.

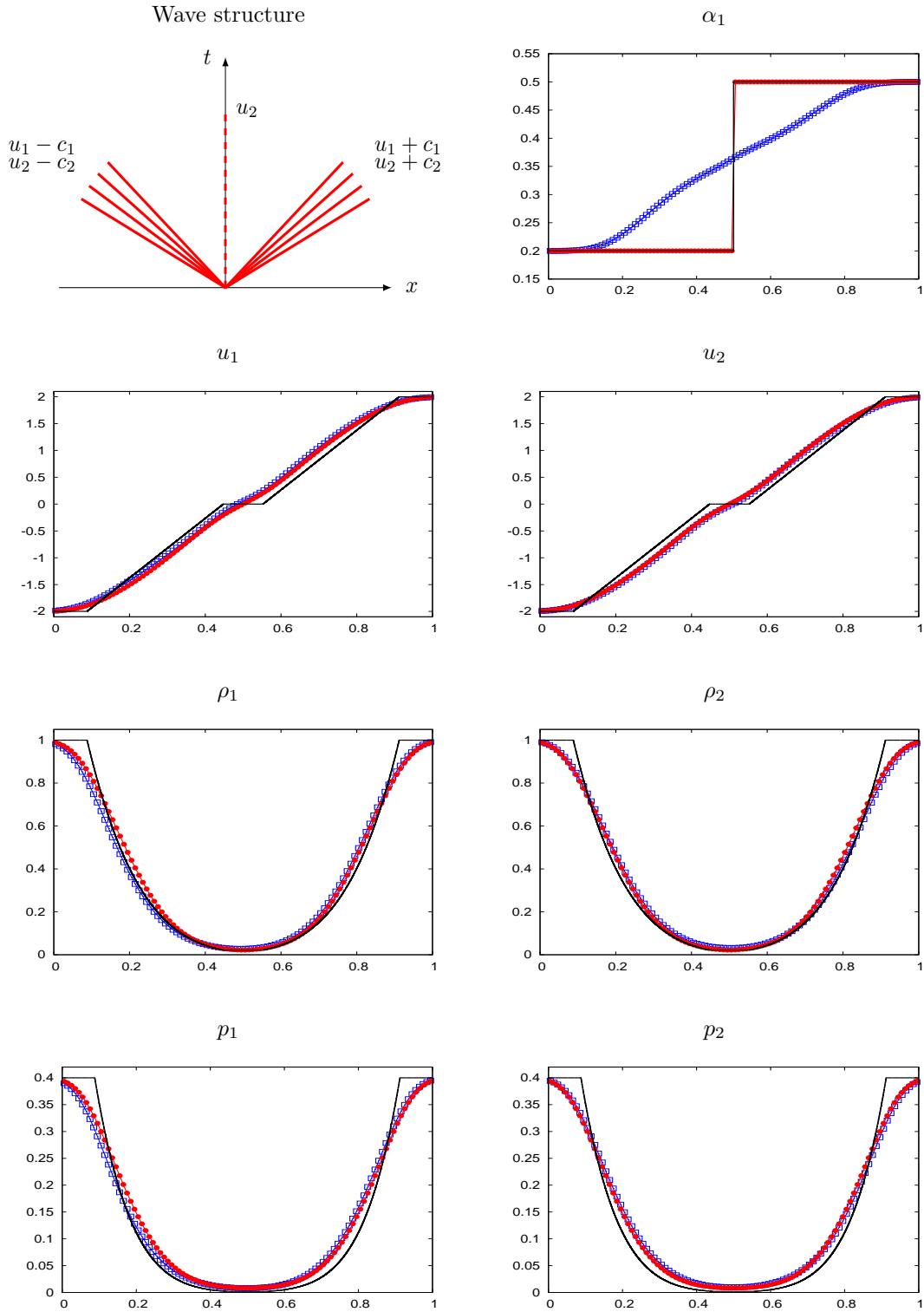


Figure 6: Test-case 3: Structure of the solution and space variations of the physical variables at the final time $T_{\max} = 0.15$. Mesh size: 1000 cells. Straight line: exact solution, bullets: relaxation scheme.

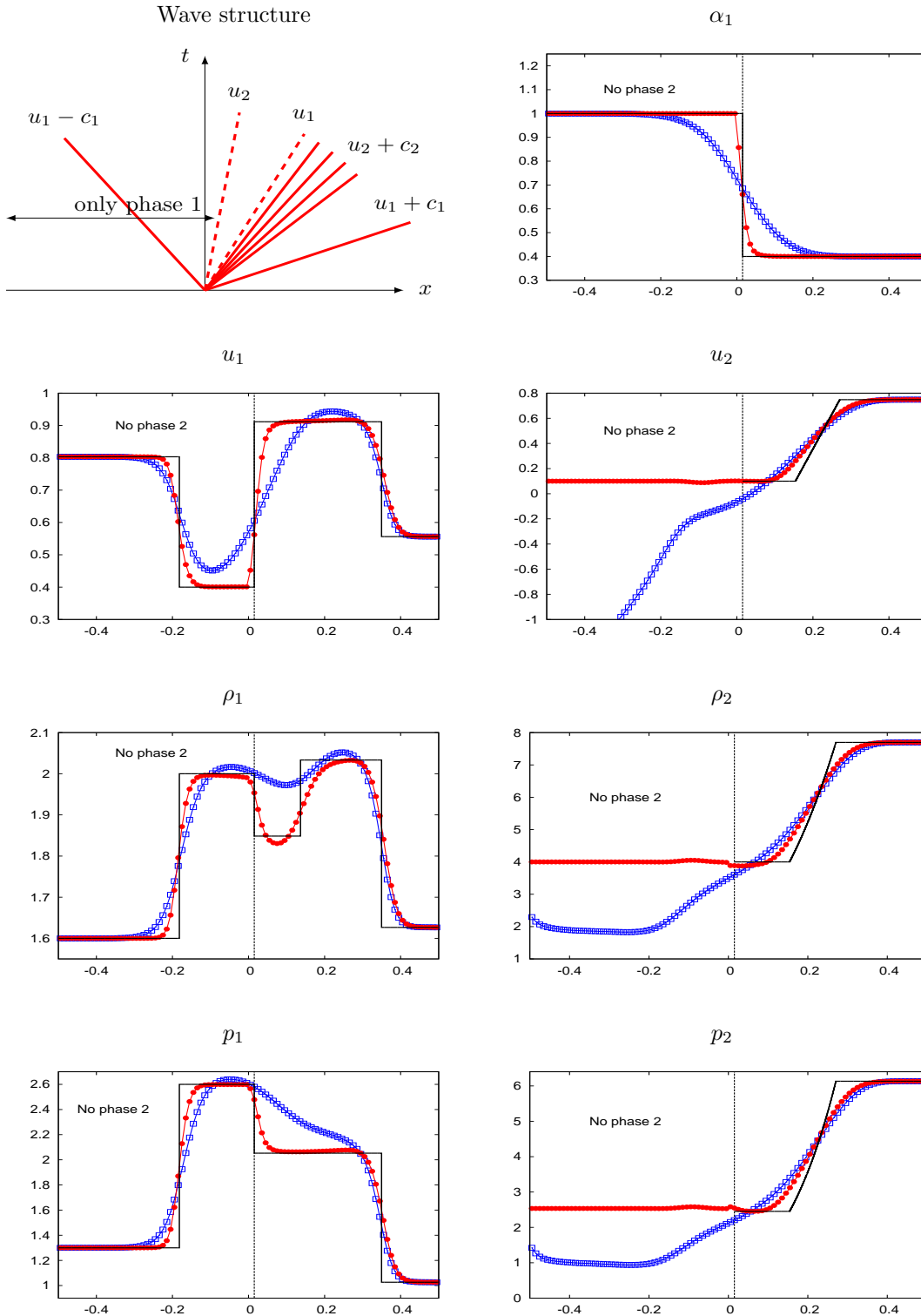


Figure 7: Test-case 4: Structure of the solution and space variations of the physical variables at the final time $T_{\max} = 0.15$. Mesh size: 1000 cells. Straight line: exact solution, bullets: relaxation scheme.

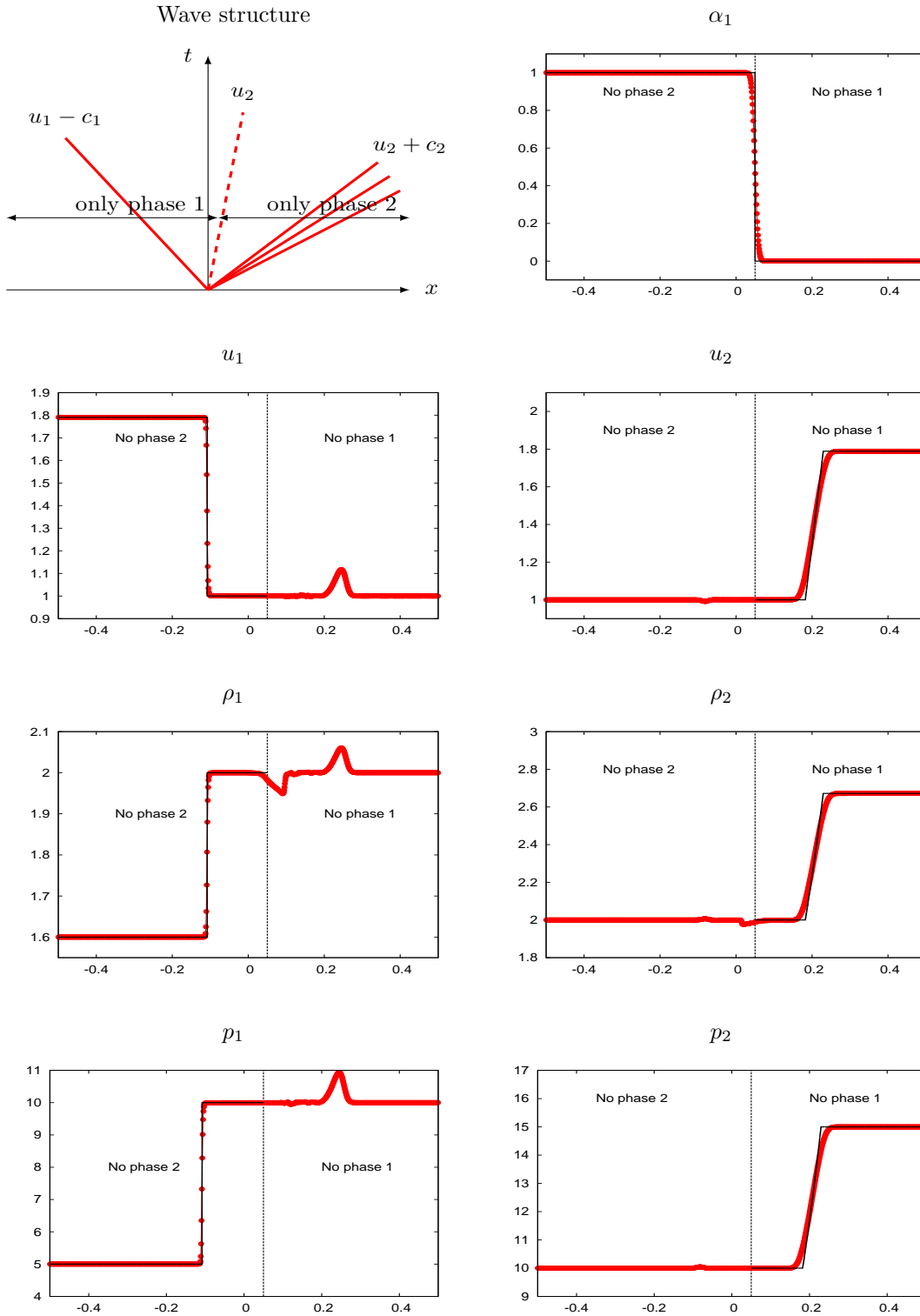


Figure 8: Test-case 5: Structure of the solution and space variations of the physical variables at the final time $T_{\max} = 0.05$. Mesh size: 1000 cells. Straight line: exact solution, bullets: relaxation scheme.